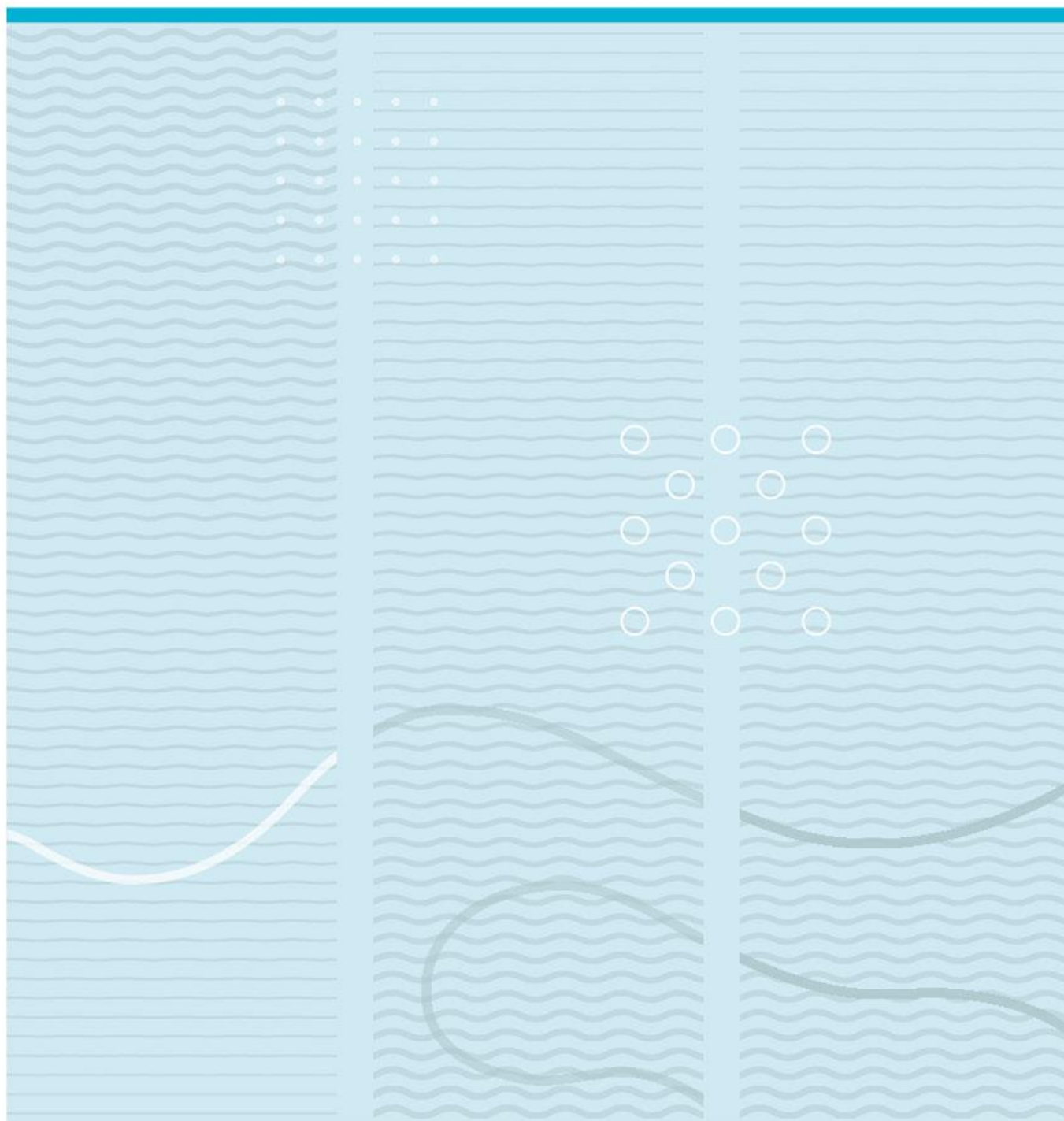


Hanna Karoline Figenschau

# Beta parapapillary atrophy

Frequency and distribution of frequencies around the optic nerve head by the means of colour fundus photography and spectral domain optical coherence tomography (SD-OCT)



University of South-Eastern Norway  
Faculty of Health and Social Science  
Institute of Optometry, Radiography and Lighting Design  
PO Box 235  
NO-3603 Kongsberg, Norway

<http://www.usn.no>

© 2019 Hanna Karoline Figenschau

This thesis is worth 30 study points

## Summary

**Purpose:** The purpose of the study was to investigate the prevalence and distribution of frequencies of beta parapapillary atrophy and its distal border around the optic nerve head identified by the means of colour fundus photographs and SD-OCT.

**Methods:** 135 eyes of 68 subjects with mean age of 61.33 years (range: 43-81, SD: 9.68) was included. Subjects underwent anamnesis and a standard optometric examination with dilated imaging of colour fundus photography and SD-OCT in both eyes. Fundus photographs was marked regarding presence of beta parapapillary atrophy and its distal border. IR-images with markings of OCT-defined distal border of beta parapapillary atrophy was overlaid fundus photos digitally before further analyses.

**Results:** Prevalence of beta parapapillary atrophy by means of fundus photography was 23.4% (CI: 13.0, 33.8) in right eyes and 27.0% (CI: 16.0, 38.0) in left eyes with an insignificant difference between eyes ( $p= 0.550$ ). Prevalence of beta parapapillary atrophy in both eyes was 21.7% (CI: 11.3, 32.1). The atrophy was most prevalent in temporal region, decreasing in inferior region before superior region, towards least frequent nasal region. The distribution of frequencies by means of SD-OCT corresponded with that of fundus photographs, but the frequencies in SD-OCT was generally higher. Overlapping distal borders of parapapillary atrophy by means of fundus photo and SD-OCT was most frequent in superior-temporal region in both eyes. OCT-defined distal border placed on the inside of fundus photo-defined distal border was most frequent in inferior-temporal region in both eyes. OCT-defined distal border placed on the outside of fundus photo-defined distal border was most frequent in superior-temporal region in both eyes. There were much higher frequencies for the OCT-defined distal border placed on the inside of fundus photo-defined distal border, than the two other outcomes, in both eyes.

**Conclusion:** The frequency and distribution of frequencies of beta parapapillary atrophy identified by means of fundus photography and SD-OCT was consistent with previous studies. Frequency and distribution of frequencies of beta parapapillary atrophy and its distal border around the optic nerve head was unique for this study and provides further clinical knowledge of parapapillary atrophy when using both image modalities.

**Key words:** Colour fundus photography, SD-OCT, beta parapapillary atrophy, distal border, prevalence and distribution.



# Contents

<b>Summary</b> .....	<b>3</b>
<b>Contents</b> .....	<b>5</b>
<b>Foreword</b> .....	<b>9</b>
<b>1 Introduction</b> .....	<b>11</b>
1.1 Morphology of sclera, choroid and retinal layers .....	11
1.2 Digital fundus photography .....	11
1.2.1 Image quality .....	12
1.3 OCT .....	13
1.4 Classification of parapapillary atrophy .....	13
1.5 Beta parapapillary atrophy .....	14
1.5.1 Prevalence .....	15
1.5.2 Distribution of frequencies around optic nerve head .....	15
1.5.3 Distal border of beta atrophy .....	16
<b>2 Purpose of study</b> .....	<b>17</b>
2.1 Research questions .....	17
2.2 Significance .....	18
<b>3 Methods</b> .....	<b>19</b>
3.1 Study design .....	19
3.2 Study sample .....	19
3.2.1 Target population .....	19
3.2.2 Study population .....	19
3.2.3 Exclusion criteria .....	20
3.3 Recruitment .....	21
3.3.1 ID-key .....	21
3.4 Execution .....	22
3.4.1 General optometric examination .....	22
3.4.2 Fundus camera .....	23
3.4.3 SD-OCT and IR-images .....	24
3.5 Analyses .....	26
3.5.1 Properties for screen .....	26
3.5.2 Image processing part I: Analyses of image quality and evaluation of presence of beta parapapillary atrophy on fundus images .....	26
3.5.3 Image processing part II: Overlapping fundus- and IR-images .....	34

3.6	Reproducibility and repeatability .....	37
3.7	Statistics .....	38
3.8	Ethics.....	39
<b>4</b>	<b>Results .....</b>	<b>41</b>
4.1	Demographics .....	41
4.2	Image quality of fundus photographs .....	42
4.3	Frequency of beta parapapillary atrophy by means of fundus photography	43
4.3.1	Frequency of beta parapapillary atrophy with total image quality grade 2 and 3 done separately .....	43
4.4	Distribution of frequencies of beta parapapillary atrophy around the optic nerve head by means of fundus photography .....	43
4.5	Distribution of frequencies of beta parapapillary atrophy around the optic nerve head by means of fundus photography and SD-OCT .....	45
4.5.1	Frequency of beta parapapillary atrophy by means of SD-OCT .....	45
4.5.2	Distribution of frequencies of beta parapapillary atrophy around the optic nerve head by means of SD-OCT .....	46
4.6	Distribution of frequencies of distal border of beta parapapillary atrophy by means of fundus photo and SD-OCT.....	47
<b>5</b>	<b>Discussion.....</b>	<b>51</b>
5.1	Frequency of beta parapapillary atrophy by means of fundus photography	51
5.1.1	Unclassified parapapillary atrophy and critical evaluation of current definition of beta parapapillary atrophy.....	53
5.1.2	Image quality of fundus photographs .....	54
5.2	Distribution of frequencies of beta parapapillary atrophy around the optic nerve head by means of fundus photography .....	56
5.3	Distribution of frequencies of beta parapapillary atrophy around the optic nerve head by means of fundus photography and SD-OCT .....	58
5.3.1	Frequency of beta parapapillary atrophy by means of SD-OCT .....	58
5.3.2	Distribution of frequencies of beta parapapillary atrophy around the optic nerve head by means of SD-OCT .....	58
5.4	Distribution of frequencies of distal border of beta parapapillary atrophy by means of fundus photography and SD-OCT.....	59
5.5	Study limitations .....	61
<b>6</b>	<b>Conclusion.....</b>	<b>63</b>

<b>References .....</b>	<b>65</b>
<b>List of figures, tables and charts.....</b>	<b>69</b>
<b>Annexes .....</b>	<b>71</b>





## Foreword

This master thesis has gotten out the best and the worst in me throughout the process, and I embrace all the new knowledge about myself and the knowledge this master thesis has given me on the topic. Mainly I want to thank Per Olof Lundmark, my supervisor and a very wise man. Thank you for guiding me throughout the process of this master thesis. I also want to thank Vibeke Sundling for having me as part of the team in the project “Diabetes Vision and Ocular Health”. It has been very interesting and educational. A special thanks goes to the “go-to person” Tove Lise Morisbakk with her kindness and support throughout these two additional years of my education. Marina Rønning, A.K.A my nearest and dearest friend and colleague: I suppose you are the reason why I never gave up, and the reason optometry seems more fun than it already is. Jan Martin Rønning, thank you for being a promotor of fun activities in the “Kongsberg-gang”. And last, but not least thank you, Esben Evanger for making me dinner and forcing me to sleep. Thank you for joining on this journey.

Kongsberg, 02.05.2019

Hanna Karoline Figenschau



# 1 Introduction

## 1.1 Morphology of sclera, choroid and retinal layers

The sclera is composed of connective tissue and can be classified into three layers from external to internal; episclera, stroma and lamina fusca, in which the latter is a more loosely packed tissue with many pigmented melanocytes, that have migrated from the vascular choroid (Bergmanson, 2014). The choroid is a highly vascular, but relatively thin, brown layer coating the internal sclera by contacting it with the suprachoroid, the external layer of choroid (Bergmanson, 2014). The suprachoroid is adjacent to a layer of large vessels, which in turn contacts with a layer of small vessels, before turning into a third, internally layer named the choriocapillaris (Bergmanson, 2014). Choriocapillaris borders to the external, elastic and fenestrated layer of Bruch's membrane, that promotes nutrition to the retina and facilitates removal of its waste products (Bergmanson, 2014). Internally cuticular layer of Bruch's borders to the basement membrane of retinal pigment epithelium (RPE) (Bergmanson, 2014). RPE-cells contain pigments of melanin and lipofuscin (Bergmanson, 2014). The outer segment of photoreceptors are placed on the RPE-cells internal side, and the inner segment of photoreceptors border to the external limiting membrane. The rest of the retinal layers are, from outermost to innermost, outer nuclear layer, outer plexiform layer, inner nuclear layer, inner plexiform layer, ganglion cell layer, retinal nerve fibre layer (RNFL) and the internal limiting membrane (Bergmanson, 2014).

## 1.2 Digital fundus photography

A common procedure in ophthalmology and optometry is digital fundus photography (Abràmoff, Garvin & Sonka, 2010; Bartling, Wanger & Martin, 2009). It is considered important in clinical practice as it provides accurate and critical documentation in evaluation of the posterior pole, especially in diagnosing and follow-up of glaucoma, diabetes and age-related macular degeneration (Bartling et al., 2009). A 2-dimentional image is created with exposure of light on the retina, which in turn reflects light back from the 3-dimentional semi-transparent tissues (Abràmoff et al., 2010; Allen & Triantaphillidou, 2012). Non-mydratiac retinal cameras, that is not dependent on dilation

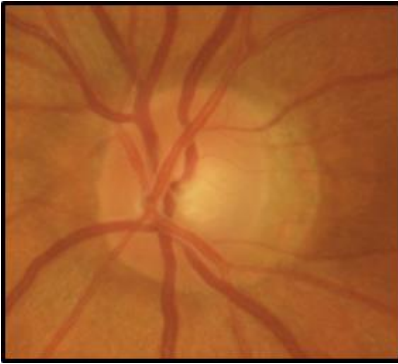


*Figure 1-1 Retinal image of optic nerve head with adjacent visible sclera surrounded by evenly coloured retina.*

of the pupils upon imaging, normally captures images with a 45-degree field of view (Morisbakk, 2014). Dilating of the pupils is recommended for high-quality fundus photos (Tyler, Saine & Bennet, 2003). Resolution of the image is dependent on the content of pixels in the image, which in turn depends on the chosen retinal camera (Allen & Triantaphillidou, 2012; Morisbakk, 2014). Planning of the image is important, by aligning and focusing the target of the image, to get optimal image quality (Tyler et al., 2003). The red appearance seen on ophthalmoscopy or imaging of the retina is owned to the choriocapillaris (Bergmanson, 2014). The pigments in the choroid absorbs stray light, while the white underlying sclera reflects light (Bergmanson, 2014), as seen by colour differences in figure 1-1.

### 1.2.1 Image quality

The retinal information from a fundus image is highly dependent on the image quality (Bartling et al., 2009). A retinal image is influenced by image quality attributes such as tone or contrast, reproduction of brightness, colourfulness and hue, resolution or reproduction of fine details, sharpness and noise (Allen & Triantaphillidou, 2012). These attributes make up the overall impression of the image quality. Image quality can be defined as “[...] the subjective impression of goodness that the image conveys” (Allen & Triantaphillidou, 2012), which means that image quality is a subjective evaluation relating to human perception, memory, experience and so on (Allen & Triantaphillidou, 2012). Therefore, in clinical practice, using a reference image is helpful in evaluating image quality during procedure of retinal imaging, as one can adjust attributes such as exposure and sharpness upon procedure (Allen & Triantaphillidou, 2012; Tyler et al., 2003). The digital resolution of an image is limited by the optical system and the human eye (Allen & Triantaphillidou, 2012; Tyler et al., 2003).

## 1.3 OCT

The imaging technology of optical coherence tomography (OCT) has improved rapidly since the first instruments, and the non-invasive in-vivo retinal imaging technique has gone from being a laboratory instrument for study purposes to be a widely used standard optometric tool in clinical practice (Huang et al., 1999; Staurenghi et al., 2014). Spectral domain (SD)-OCT obtains cross-sectional images of retinal layers with high speed by using a super luminescent diode, a low coherent infrared laser of 800-870 nanometres (nm), that reflects the light from the different retinal layers when the beam is pointed on the retina (Huang et al., 1991; Morisbakk, 2014). The histology of the sclera, choroid, retinal layers and optic nerve head can be seen by the means of SD-OCT, with different tissue layers being hyper- or hypo reflective (Staurenghi et al., 2014).

## 1.4 Classification of parapapillary atrophy

Parapapillary atrophy is divided into alpha, beta and gamma, and are often referred to as zones, by their location adjacent to the optic nerve head. Their features and appearance are different and can be observed on both fundus photographs and SD-OCT (Dai, Jonas, Huang, Wang & Sun, 2013). Beta parapapillary atrophy will be described in chapter 1.5. Ophthalmoscopically, features of alpha zone is irregular hypo-and hyperpigmentation seen on ophthalmoscopy (Jonas, Nguyen, Gusek & Naumann, 1989; Jonas et al., 2003; Ramrattan, Wolfs, Jonas, Hofman & de Jong, 1999; Wang, Xu, Yang, Ma, & Jonas, 2008), which corresponds histologically with nonuniform sized RPE-cells and granuled melanin content (Curcio et al., 2000; Kubota et al., 1993). The alpha zone borders to the scleral ring of Elsching centrally if beta and gamma is not present, and to the rest of the healthy retinal tissue peripherally (Jonas et al., 1989; Ramrattan, 1999). Ophthalmoscopically, the appearance of beta and gamma cannot be differentiated but the SD-OCT shows that beta has Bruch's membrane, while gamma is devoid of this layer (Dai et al., 2013). Histologically, and in OCT, gamma correlates with a marked elongated sclera with overlying RNFL and is always located adjacent to the optic nerve head (Dai et al., 2013; Jonas et al., 2012; Zhang, Wang, Wei, Xu & Jonas, 2018).

There is some controversy in the pertinent literature about associations of the different types of atrophy. Presence of beta is strongly associated with the presence of alpha (Dai et al., 2013; Jonas et al., 2003). Presence of beta and gamma are not directly dependent on each other (Vianna et al., 2016). Mainly, higher prevalence of beta parapapillary atrophy is associated with glaucoma and higher prevalence of gamma parapapillary atrophy is associated with myopia and axial elongation. (Dai et al., 2013; Kim, Kim, Weinreb & Lee, 2013; Miki et al., 2017; Zhang et al., 2018). There is no evidence in pertinent literature that diabetes mellitus is associated with beta parapapillary atrophy (Guo, et al., 2012; Kim et al., 2013; Zhang, 2018).

## **1.5 Beta parapapillary atrophy**

Features of beta zone is marked atrophy or absence of RPE, marked atrophy of choriocapillaris, thinning of chorioretinal tissues and a crescent-shape distal and central border (Guo et al., 2012; Jonas, et al., 1989; Jonas et al., 2003; Ramrattan et al., 1999; Wang et al., 2008). These features are ophthalmoscopically seen as visible sclera with large choroidal vessels (Dai, et al., 2013; Guo, et al., 2012; Jonas, et al., 1989; Jonas et al., 2003; Lee, et al., 2011; Ramrattan, et al., 1999; Wang, et al., 2008). The zone of beta is anatomically localized and bordered between the central optic nerve head's external wall of scleral ring of Elschnig, and the peripheral alpha zone if present-, or the rest of the retina if alpha is not present (Dai, et al., 2013; Guo, et al., 2012; Jonas, et al., 1989; Jonas et al., 2003; Lee, et al., 2011; Ramrattan, et al., 1999; Wang, et al., 2008). Histologically, the mentioned features of beta zone correspond with a denuded Bruch's membrane in terms that it is lacking RPE, and density of photoreceptors are markedly reduced or completely missing (Curcio et al., 2000; Kubota et al., 1993). This is also seen on a cross-section of OCT, where the hyperreflective band of RPE/Bruch's complex is missing the RPE, and Bruch's membrane is left as a single hyperreflective layer (Dai et al., 2013; Hayashi et al., 2012; Lee et al., 2010; Zhang, et al., 2018). The hyperreflective IS/OS junction determinates peripherally to the distal border of beta parapapillary atrophy, and deeper retinal layers from ganglion cell layer to outer nuclear layer may be absent or seen as fragments in the beta area (Hayashi et al., 2012; Lee, et al., 2010). In a cross-sectional OCT image, where the gamma and beta atrophy can be differentiated, the gamma is always centrally placed if present (Dai et al., 2013; Zhang et al., 2018).

### 1.5.1 Prevalence

There are many studies on prevalence of beta parapapillary atrophy in the pertinent literature, but only a few studies are based on a normal population. For the relevance of this study, only the normal population-based studies are discussed. Ophthalmoscopic studies, using fundus photography varies in prevalence from studies using OCT. The first study on prevalence of beta parapapillary atrophy using fundus photographs was done by Jonas et al., (1989) who found a prevalence of 15.2% in eyes. Ramrattan et al. (1999) found a prevalence of 13.0% in at least one eye. Jonas et al. (2003) found a prevalence of 11.4% of eyes. The highest prevalence was reported by Wang et al (2008) with a prevalence of 19.9%. The difference in prevalence in the different studies might be explained by differences in number of included subjects, age differences, differences in ethnicity and differences in range of refractive powers.

For beta parapapillary atrophy observed by the means of OCT, the prevalence ranges between 75.0% in at least one normal eye (Lee et al., 2010), 63.0% in one eye (Hayashi et al., 2012) and 72.6% of eye (Zhang et al., 2018). Difference in number of subjects and range of refractive powers might explain some of the difference.

### 1.5.2 Distribution of frequencies around optic nerve head

Jonas et al. (1989) is also the first study in measuring the prevalence of beta parapapillary atrophy distributed around the optic nerve head, observed on fundus photography. They found that the beta parapapillary atrophy was most frequent in areas of the following order: temporal, inferior-temporal, superior-temporal and nasal. Wang et al (2008) found the same order for distribution of frequencies. Jonas et al. (2003) found that there was no difference in frequencies between temporal, inferior-temporal and superior-temporal sections, but nasal section was least frequent.

There is only one study regarding distribution of frequencies of beta parapapillary atrophy by means of OCT. Zhang et al (2018) found that parapapillary atrophy was most frequent in areas of the following order: temporal, inferior, superior and nasal (Zhang et al., 2018).

### 1.5.3 Distal border of beta atrophy

The distal border of the beta parapapillary atrophy has been proven to be easy to define and mark on fundus photographs in a study on interobserver variation in measurements of beta peripapillary atrophy in glaucoma (Tuulonen, Jonas, Välimäki, Alanko & Airaksinen, 1996). The distal border has also been proven to be easy to detect on OCT (Park, De Moares, Tello, Liebmann, Ritch, 2010). Literature is sparse when it comes to concordance of beta parapapillary atrophy's termination of distal border between fundus photo and OCT. Park et al. (2010) found that in 65.0% of cross-sectional Fourier-Domain-OCT images of the distal border of beta parapapillary atrophy, the borders overlapped on OCT and fundus photography (Park et al., 2010). In 35.0% of sections, the distal border on OCT was placed on the inside of the fundus photo-defined distal border (Park et al., 2010). The cause was suggested to be that Bruch's membrane was not entirely denuded of RPE on OCT-images, which is most likely not visible ophthalmoscopically (Park et al., 2010).



## **2 Purpose of study**

The purpose of the study was to investigate the prevalence and distribution of frequencies of beta parapapillary atrophy and its distal border around the optic nerve head identified by the means of colour fundus photographs and SD-OCT.

### **2.1 Research questions**

The purpose of the study was based on these research questions:

- In a sample of diabetic adults over the age of 40 years, what is the frequency of beta parapapillary atrophy identified by means of fundus photography in one and both eyes?
- In eyes with beta parapapillary atrophy identified by means of fundus photography, what is the distribution of frequencies of beta parapapillary atrophy observed surrounding the optic nerve head?
- In eyes with beta parapapillary atrophy identified by means of either fundus photography or SD-OCT, what is the distribution of frequencies of beta parapapillary atrophy observed on both imaging modalities surrounding the optic nerve head?
- In eyes with beta parapapillary atrophy identified by means of both fundus photography and SD-OCT, what is the distribution of frequencies of beta parapapillary atrophy with an overlapping fundus photo- and OCT- defined distal border of the beta parapapillary atrophy observed surrounding the optic nerve head?
- In eyes with beta parapapillary atrophy identified by the means of both fundus photography and SD-OCT, what is the distribution of frequencies of beta parapapillary atrophy with an OCT-defined distal border located on the inside of the fundus photo-defined distal border of the beta parapapillary atrophy, observed surrounding the optic nerve head?

- In eyes with beta parapapillary atrophy identified by the means of both fundus photography and SD-OCT, what is the distribution of frequencies of beta parapapillary atrophy with an OCT-defined distal border located on the outside of the fundus photo-defined distal border of the beta parapapillary atrophy, observed surrounding the optic nerve head?

## **2.2 Significance**

The study was expected to improve our understanding of the frequency and distribution of frequencies of beta parapapillary atrophy and its distal border surrounding the optic nerve head by means of colour fundus photography and SD-OCT. Beta parapapillary atrophy can be identified on both image modalities and is linked with development of glaucoma. Therefore, it is clinically relevant to identify the beta parapapillary atrophy and its distal border and to monitor it over time with image documentation. Fundus photo and OCT is common instruments in clinical practice, although the latter is less integrated in routine use. Both image modalities can distinguish between alpha and beta parapapillary atrophy, although gamma parapapillary atrophy is only seen with OCT. The image modalities complement each other in general diagnosing in optometric practices, but regarding beta parapapillary atrophy the relevance of the image modalities in clinical practice is sparse in the pertinent literature. To my knowledge, no studies have investigated the frequency and distribution of frequencies of beta parapapillary atrophy and its distal border around the whole optic nerve head in both eyes on fundus photographs and SD-OCT in the same study.

## **3 Methods**

This study is part of a larger prospective, cross-sectional study “Diabetes, vision and ocular health” (DVOH). A large amount of data was collected, but only the measurements and demographics of relevance was selected for this study. Optometric procedures were standardized, and excessive training in instrumentation was given by supervisors (V.S., T.L.M., P.O.L.) according to standard protocols (Annex 2 and 3), and recruitment and execution was done collaborating with four other observers of the main project DVOH (M.R., J.L.P., S.S., J.A.). Analyses of the SD-OCT-scans and IR-images was done by a secondary observer (M.R.) to secure a blind design for the main observer (H.K.F) when analyzing fundus photographs in this study, before comparing them with SD-OCT results.

### **3.1 Study design**

The study is a cross-sectional study.

### **3.2 Study sample**

#### **3.2.1 Target population**

The target population is males and females above the age of 40 years in Norway.

#### **3.2.2 Study population**

Subjects eligible to the study was males and females above the age of 40 years with type 2 diabetes, who participated through the main study DVOH at the clinic at the University of Southeast Norway, campus Kongsberg, during the period from 1<sup>st</sup> of august 2018 to 28<sup>th</sup> of January 2019.

### 3.2.3 Exclusion criteria

Subjects were excluded from the study if fundus images were missing for both eyes.

One eye would be excluded if a fundus image was missing.

An image would be excluded from some or all the image analyses in these cases:

- Total fundus image quality is poor; no possibility of evaluating the structures within the relevant area and therefore the whole image. Poor quality is equal to “Grade 1” in table 3-3.
- Missing IR-image (or cross-sectional OCT image).
- Inadequate image quality of the IR-picture; land marks not visible, inhibiting procedure of overlapping IR-image and fundus photograph.
- Dislocation of cross outside the papillae on IR-image.

Radial sections would be excluded from the analyses of evaluating presence of beta parapapillary atrophy in these cases:

- Covering of relevant areas; no possibility of evaluating parts of structures within the relevant area due to retinal blood vessels or floaters in the specific directional section.
- Dislocation of the centre of the radial scan pattern in the IR-picture, located beyond the border of a papillae-centered circle with a diameter 20% of the papilla size. All sections would be excluded except the section in the direction of the misalignment and one section immediately adjacent to each side.

Radial sections would be excluded from the analyses of evaluating the distal border of the parapapillary atrophy in these cases:

- Dislocation of the centre of the radial scan pattern in the IR-picture, located beyond the border of a papillae-centered circle with a diameter 20% of the papilla size. All sections would be excluded except the section in the direction of the misalignment and one section immediately adjacent to each side.
- Inadequate image quality of the cross-sectional OCT-images; no possibility to differentiate between the retinal layers in the parapapillary area.
- Shadowing of the cross-sectional OCT-images; no possibility to differentiate between the retinal layers in the parapapillary area because the border of the atrophy cannot be seen.

### 3.3 Recruitment

The recruitment of subjects to this study was done via the main project “DVOH”. Recruitment and booking for this study were executed between 1<sup>st</sup> of August and 3<sup>rd</sup> of December. Participation was voluntary for any person above 18 years with diabetes type 2. Information about the study was given via the home page of the University (Universitetet i Sørøst-Norge), articles and notes in a local and a national newspaper, in a journal for Norwegian optometrists (Olsen, 2018) and through posters in the university clinic and in doctors’ offices in Kongsberg. This information was shared by supervisors (V.S., T.L.M.), who also would hold presentations about the study, in which one was held at the diabetes association’s premises in Buskerud. E-mails was also sent out to the optometric shops in the counties Buskerud, Vestfold and Telemark. The emails were encouraging the optometrist to give information about participating in the study to any patient with type 2 diabetes that they would examine. After approximately one month, these optometric shops were called by observers (H.K.F., J.L.P., M.R., S.S.) to follow up the email and talk to them regarding any questions about the study. Subjects who wanted to participate contacted the supervisors (T.L.M., V.S.) via email or telephone, and would then receive written information (Annex 1) about the study before they were contacted by main observer (H.K.F.) and second observer (M.R.) via telephone to schedule for examination and talk to them about any questions regarding execution. A participant was considered included when a consent form (Annex 1) in the same piece of written information was signed by the subject and the operator between the inclusion date and the examination date.

#### 3.3.1 ID-key

An anonymization was done for each subject, by randomly allocating an ID-number between 1 and 70 to each subject instead of using their own identification. An ID-key made in excel connected their allocated ID-number and journal number. Only the journal number in the ID-key could re-connect with personal information belonging to the data that was locally stored on a password-protected computer in a lab with limited access for this study. The ID-key was digitally stored in a storage unit called “Figshare”. Access was limited to only two observers (H.K.F., M.R.) for their respective sub-studies, and the manager of the main study “DVOH”, where all had a personalized username and password to log in. Password and username will be deleted

after the study is done, and the ID-key will be kept under the main supervisor's responsibility. The ID-key is illustrated in figure 3-1.

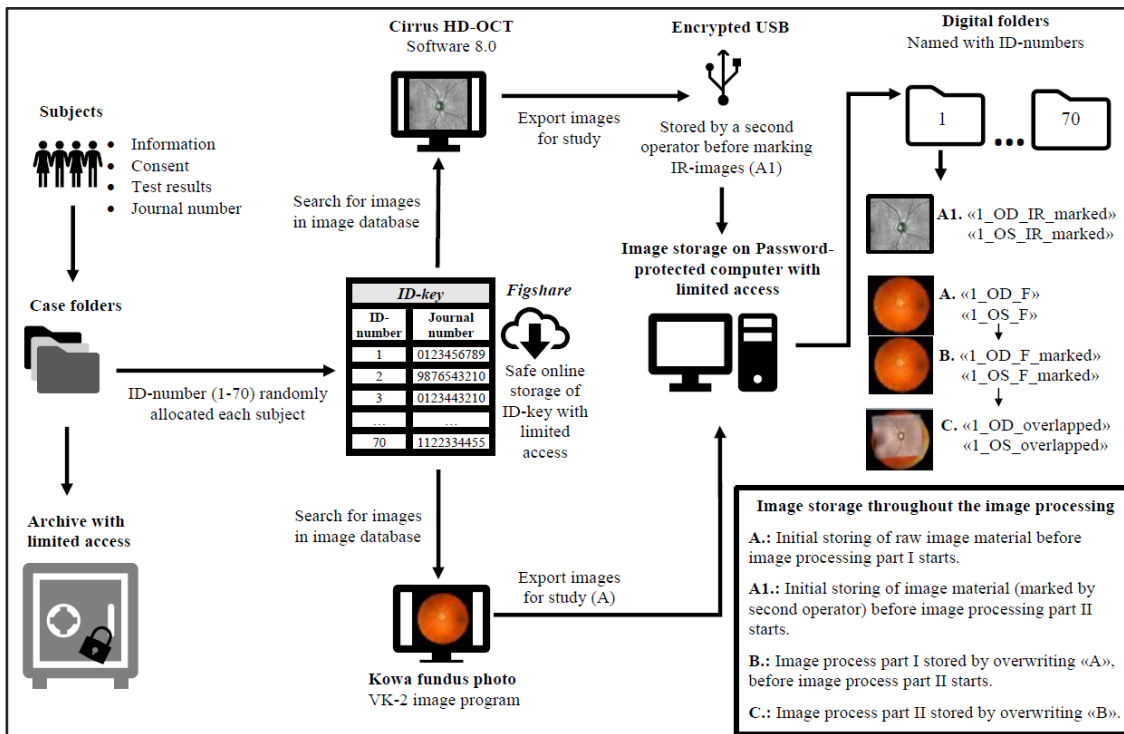


Figure 3-1 Data storage. The figure gives an overview of the storage of data throughout the process from data collection to analyses.

### 3.4 Execution

#### 3.4.1 General optometric examination

As mentioned, there were 5 observers cooperating in data collection (J.L.P., J.A., M.R., S.S., H.K.F). Full name, contact information, information about subjects and test results from each subject was noted in a booklet and kept in an individual case folder for each subject, and stored in a locked archive closet with only supervisors and observers from DVOH being able to access. Each observer was responsible for gathering all information and test results needed for the main study and sub study, according to protocols of DVOH. The examination consisted of an extended standardized optometric procedure, with anamneses, initial testing, refraction and thorough evaluation of anterior and posterior segment and visual function. Dilating topicals was used (Tropicamide Minims 0.5%) before posterior segment instrumentation was conducted. For this study, the fundus camera and SD-OCT was of relevance, along with binocular subjective

refraction and demographics like gender, age and any self-reported diagnose of ocular disease.

### 3.4.2 Fundus camera

#### 3.4.2.1 *Specifications*

A standardized protocol for fundus camera was followed and was always available during data collection (Annex 2). Fundus images were obtained in a dark room with Kowa Nonmydriatic retinal camera (model WX 3D, image software version VK-2, Kowa Company, Ltd., Japan) with an attached Nikon digital SLR camera (model D90, Nikon Corporation). The resolution of the attached digital camera is 13.3 mega pixel (MP) (Nikon Corporation, 2008). The fundus image dimensions were 4288 (pixels in width) x 2848 (pixels in height) with a resolution of 94 PPI, a 24-bit colour depth, an RBG colour channel (8bpc) and with a tolerance of pixel pitch (digital resolution) on fundus of 4.5 microns +/- 7% (Kowa Company, 2010; Niko Corporation, 2008). The light source is a near-infrared LED light for illuminating the retina while aligning and focusing the image. A xenon flash lamp of light is used to illuminate the retina to form the photograph (Kowa Company, 2010).

#### 3.4.2.2 *Procedure*

The program used was “Normal Disc” with an internal fixation point projected nasally in the patient’s visual field for the eye of footage, forming an image with visual field of 45 degree with the optic nerve head in the centre. Images was manually aligned by observing the eye on an LCD monitor. Normal pupil mode was used, and if needed, the mode “Small pupil” could be used, and gained the same visual field of the image as normal mode. After aligning the camera in the anterior segment, the posterior segment was aligned and focused. One optimal picture from each eye was obtained, in terms of alignment, sharpness and exposure. If the picture quality was insufficient, new images was obtained by optimizing the insufficient factors. For further description of the procedure, see Annex 2.

#### 3.4.2.3 *Image storage*

For this study, the subject’s fundus photographs were exported from the image software “VK-2” and stored as tiff-files on a local password-protected computer, in a lab with

limited access (figure 3-1) (see Annex 4 for exporting of images). The journal number from the ID-key was used to search for each subject in the image program. For each subject the best image available was subjectively chosen for each eye and was exported to a digital folder named the same as the current subjects allocated ID-number (e.g.: “1”, “2”, “3” etc.). Each image was named, as example, “1\_OD\_F” for right eye and “1\_OS\_F” for left eye for subject with ID-number 1 (figure 3-3).

### 3.4.3 SD-OCT and IR-images

#### 3.4.3.1 Specifications

A standardized protocol for SD-OCT was followed and was always available for all observers during data collection (Annex 3). Cross-sectional OCT images with belonging IR-images were obtained in a dark room with the use of Cirrus HD-OCT (model 5000, software version 8.0, Carl Zeiss Meditec, Inc., Dublin, CA). The instrument uses an 840-nanometre wavelength super luminescent diode with scan speed of 27 000 A-scans per second to obtain cross-sectional images. Axial and transverse resolution in tissue is 5.0 and 15.0 microns, respectively, and depth of the A-scans in tissue is 2.0 mm (Carl Zeiss Meditec, 2014). The program used was “HD radial”, a composite of 12 high-definition radial scan lines, in which each line contains 8 B-scans, and each B-scan is made of 1024 A-scans. IR-images dimensions were 1109 x 924. The 12 lines makes a radial pattern by their separation of 15 degrees (figure 3-2: left). A live observation of the fundus is made possible with infrared light, and the radial pattern can be moved to desired location on the fundus.

#### 3.4.3.2 Procedure

12 cross-sectional images were obtained from each eye, with a belonging infrared image that indicated where the 12 cross-sectional images were located at the fundus (figure 3-2). By moving internal fixation target one step to the nasal side of the patients’ visual field, relative to the eye that was examined, the HD Radial scan centered over optic nerve head. The scan pattern could be further adjusted and dragged manually to the geometrical centre of the optic nerve head if needed. Figure 3-2 (left) shows a perfectly centered radial scan. If patients had poor fixation ability, this procedure would be difficult. Line number 1 of the scan went through the nerve heads geometrical centre in the located direction at 180 degree through 0 degree (figure 3-2) with the line itself representing the geographic place of where the cross-sectional image was obtained



from. The 12 cross-sectional images were 6 millimetres long and numerated from 1 to 12 by default. By observing the LCD screen, the posterior segment could be aligned, until the optic nerve head and its parapapillary area was centered and focused with the radial pattern centered above. Quality check of the pictures was subjectively done, along with the criteria that the quality indicator had to be 6 or stronger. New images were taken if necessary. For further description of the procedure, see Annex 3.

#### 3.4.3.3 Image storage

IR-images with belonging cross-sectional OCT images was exported from Cirrus HD-OCT to an encrypted USB by a second observer (M.R.). The same ID-key on “Figshare” was used to pick the subjects from the instrument as described above. The ID-number connected to each subject was the same for both IR-images and fundus images. When second observer (M.R) had processed the OCT-scans and IR-images in the image analyzing process, by marking the distal border of beta parapapillary atrophy on the IR-image (as described in chapter 3.5.5), the marked IR-images was exported from the encrypted USB held by the second observer, to one folder named “OCT\_IR\_marked\_HKF”, stored locally on the same computer as described above for fundus photos. The name for each IR-image had the same system as described above for the fundus images. As an example, IR-images was named “1\_OD\_IR\_marked” for right eye of subject with ID-number 1 (figure 3-3).

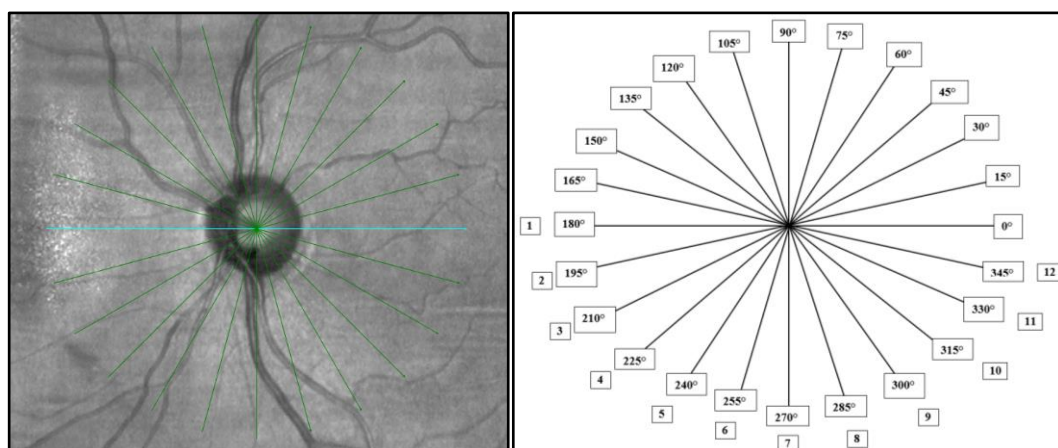


*Figure 3-2 Illustration of infrared image. Left:* Cirrus HD-OCT program “HD radial” with a papillae-centered radial cross. **Right:** Illustration of the radial cross in 15-degree separation between lines. The lines are named from 1 to 12 by default as shown in the illustration, corresponding to 12 different cross-sectional OCT-images. For this study, each section was named by its degree.

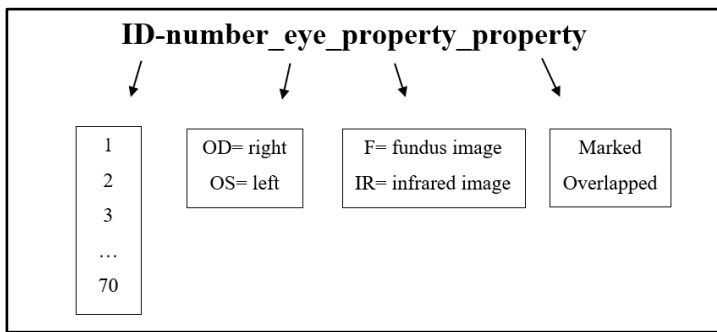


Figure 3-3. Combinations of names for images saved in different stages throughout the analyses.

### 3.5 Analyses

#### 3.5.1 Properties for screen

Room illumination for the subjective analyzing of images was set to 200-250 lx. The screen used was “EIZO ColorEdge CG277” (EIZO corp., Japan), a 27-inch LCD monitor with a resolution of 2560 x 1440 (109 pixels per inch (PPI)), 10-bit colour depth, RGB colour channels, colour temperature of 6500K and luminance of 300 cd/m<sup>2</sup>. Colour calibrating was done with “ColorNavigator 7” with the use of a built-in sensor/calibrator on the screen before each session of image analysis.

#### 3.5.2 Image processing part I: Analyses of image quality and evaluation of presence of beta parapapillary atrophy on fundus images

Fundus images were analyzed within the picture editing program Adobe Photoshop Elements (Adobe version 17.0, 2019) with 100% magnification, as one image pixel corresponds to one monitor pixel at this magnification, meaning that all pixels in the image were seen within the area on the monitor (Anon & Anon, 2010). Images was analyzed in different layers for any changes and editing of images done in the program. By saving every layer of editing, it was always possible to track back to any step in the image processing, all the way back to the raw image. For the fundus photo analyses, first the right eye was processed and saved as followed, before left eye. The tiff-image was opened in Adobe Photoshop Elements and duplicated. The original background image was never to be edited and was made invisible as a layer. The duplicated layer

was laid over the original layer and named “Quality”. In this layer, the level of lighting was subjectively optimized within the program, before evaluation of image quality for fundus photographs was registered.

### 3.5.2.1 Grading scale for image quality

A grading scale for image quality was made, as seen in table 3-1. The grading system was based on similar grading scales by Morisbakk (2014) and Lamirel et al. (2012) and was further developed and simplified to a three-grade scale with the optic disc and parapapillary area in focus on fundus photographs for this study. The image quality was evaluated based on criteria for the structure’s visibility within the relevant area, according to sharpness and exposure of light. Sharpness, exposure and total image quality was graded according to table 3-1. The three variables could be scored as “Grade 1 – poor quality”, “grade 2 – intermediate quality” or “grade 3 – good quality”. The total image quality was graded based on the sharpness and exposure, where the lowest grade of the two variables, would make the total image quality grade. The three variables of image quality were manually registered in the registration form (Annex 5).

*Table 3-1 Grading scale of total image quality.* The table shows the criteria for grading the total image quality within relevant area, based on sharpness and/or exposure. The poorest grading for sharpness and exposure is the value for chosen total image quality. Gradings are from 1-3; where grade 1= poor quality, grade 2= intermediate quality and grade 3= good quality.

	<b>Relevant area</b>	<b>Structures in relevant area</b>	<b>Grade 1</b>	<b>Grade 2</b>	<b>Grade 3</b>
<b>Sharpness criteria</b>	Defined as the optic disc rim and its parapapillary area.	Mainly defined as the smallest blood vessels; large capillaries at optic disc rim, and secondary any retinal nerve fibre layer and parapapillary atrophy and its distal border.	<i>All structures within the relevant area are not detectable, due to a total unsharp picture within relevant area.</i>	<i>Some structures or all structures within the relevant area are detectable, due to a partially unsharp picture within relevant area.</i>	<i>All structures within the relevant area are detectable, due to an optimal or close to optimal sharpness of picture within relevant area.</i>

<b>Exposure criteria</b>	Defined as the smallest blood vessels at optic disc rim, any retinal nerve fibre layer and any parapapillary atrophy and its distal border, according to the definition described elsewhere in this chapter	<i>All structures within the relevant area are not detectable, due to clearly over-/under exposure of the relevant area.</i>	<i>Some structures or all structures within the relevant area are detectable, due to uneven brightness of parts of relevant area, and/or some degree of over-/under exposure of the relevant area.</i>	<i>All structures within the relevant area are detectable, due to even brightness and no over-/under exposure of the relevant area.</i>
<b>Total image quality</b>		<i>No possibility of evaluating the structures within the relevant area with certainty.</i>	<i>Possible to do an evaluation of structures within the relevant area with some certainty.</i>	<i>Possible to do evaluation of structures within the relevant area with certainty.</i>

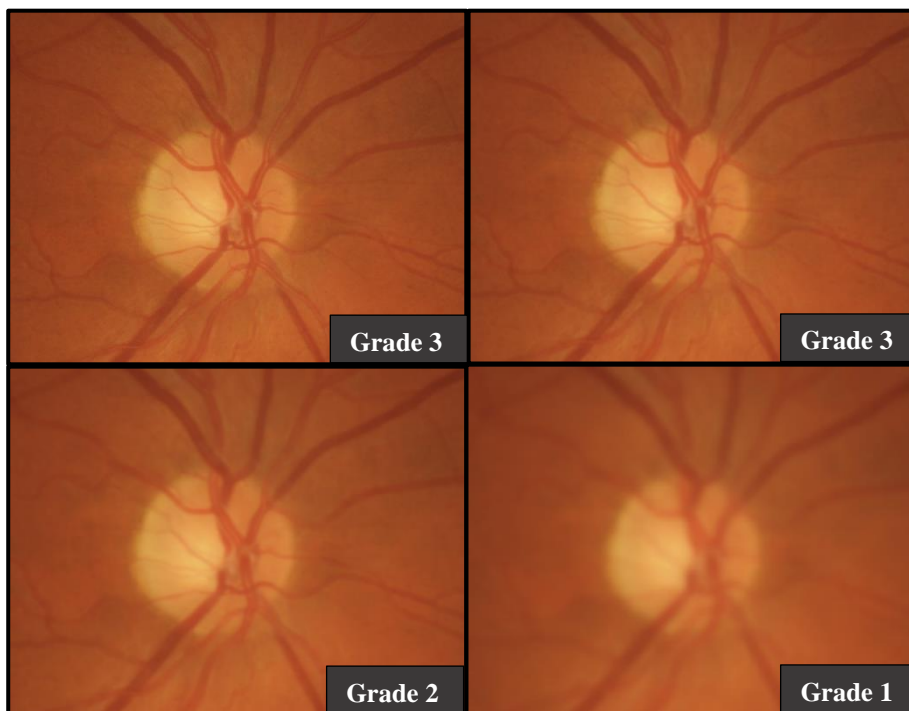


Figure 3-4 Example images for thresholds for sharpness grade 1-3 in fundus photographs, when exposure is optimal. **Upper left:** Grade 3 as all structures are detectable due to an optimal sharpness of image. **Upper right:** Grade 3 as all structures are detectable due to a close to optimal image. **Lower left:** Grade 2 as some structures

are detectable (smallest vessels on disc and RNFL details are undefined) due to a partially unsharp image. **Lower right:** Grade 1 as all structures are not detectable due to a total unsharp image. Only the large arterioles and venules are visible, and there is no possibility of determining any structures with certainty due to a poor total image quality.



*Figure 3-5. Example images for thresholds for exposure grade 1-3 in fundus photographs, when sharpness is optimal. **Upper left:** Grade 3 as all structures are detectable due to an even brightness with no over-/under exposure of image. **Upper right:** Grade 3 as all structures are detectable due to an even brightness with no under-exposure and close to no over-exposure of image. **Lower left:** Grade 2 as some structures are detectable (smallest vessels over the cup-area and centrally disc rim is undefined) due to even brightness but some degree of over-exposure of image. **Lower right:** Grade 1 as all structures are not detectable due to clearly over-exposure of the image. Only the large arterioles and venules are visible, and there is no possibility of determining any structures with certainty due to a poor total image quality.*

### 3.5.2.2 *Defining beta parapapillary atrophy and its distal border on fundus photographs*

To define the presence of beta parapapillary atrophy and to mark its distal border, another layer was created by duplicating the “Quality”-layer and rename it “Marked” in Photoshop Elements. After the analyses of the image were done for one eye, as described underneath in this chapter, all the layers with processed images were saved by overwriting the initial image saved in the digital folder and named as for example: “1\_OD\_F\_marked” (figure 3-3), for right eye of subject with ID-number 1. This process is also illustrated in figure 3-1. Note that the marked layer was made invisible before saving, as the overlapping procedure described in chapter 3.5.5 had to be done blinded for interpretation of any markings of beta parapapillary atrophy.

Based the appearance of beta parapapillary atrophy on colour fundus photography, beta parapapillary atrophy was for this study defined as a whitish or bright yellowish area, sometimes blending in with smaller or bigger darker patches within the same area, with transparency to one or several large visible choroidal vessels within parts or the whole beta zone (figure 3-6). The appearance of beta zones was compared with and distinguished from any alpha parapapillary atrophy which would be adjacent to the beta zone’s distal border and appeared less transparent and more irregularly hyper- and hypopigmented (Table 3-2). If alpha was not present, the appearance of beta would be compared and distinguished from normal retinal tissue adjacent to the beta zone’s distal border. The beta zone was also compared with and distinguished from the central border scleral ring of Elschnig who appeared as a white or brighter yellowish even shaped band bordering the optic disc rim when visible (figure 3-6), and when not visible, the disc rim itself would appear as the beta zone’s central border.

Visible choroidal blood vessels of the beta zone were defined as exposed large blood vessels of the choroidal layer, due to devoid of overlying retinal tissue, and often appeared less defined in terms of colour and sharpness, than overlying retinal blood vessels. Their directional shape was often more random curved in opposition to the straighter directional shape of retinal vessels, or radially directed away from the optic disc. Example of choroidal blood vessels are shown in figure 3-6.

The distal border of beta parapapillary zone was defined as the immediate transition between the beta zones characteristic appearance, and the adjacent alpha zone if present, and normal-variaded retinal tissue if alpha was not present (figure3-6).

Whenever a parapapillary zone could not be identified as normal retina, beta parapapillary atrophy or alpha parapapillary atrophy, nor parts of the scleral ring, and the zone would appear atrophic, it was defined as unclassified parapapillary atrophy. Comparison of this type of atrophy with beta and alpha parapapillary atrophy is shown in table 3-2. An example of unclassified atrophy is shown in figure 3-6. This type of unclassified atrophy was always placed in the same zone as the beta parapapillary atrophy would have been. Its distal border was defined as the immediate transition between the unclassified zones unfamiliar appearance, and the familiar zone of alpha parapapillary atrophy if present, and normal-variaded retinal tissue if alpha was not present.

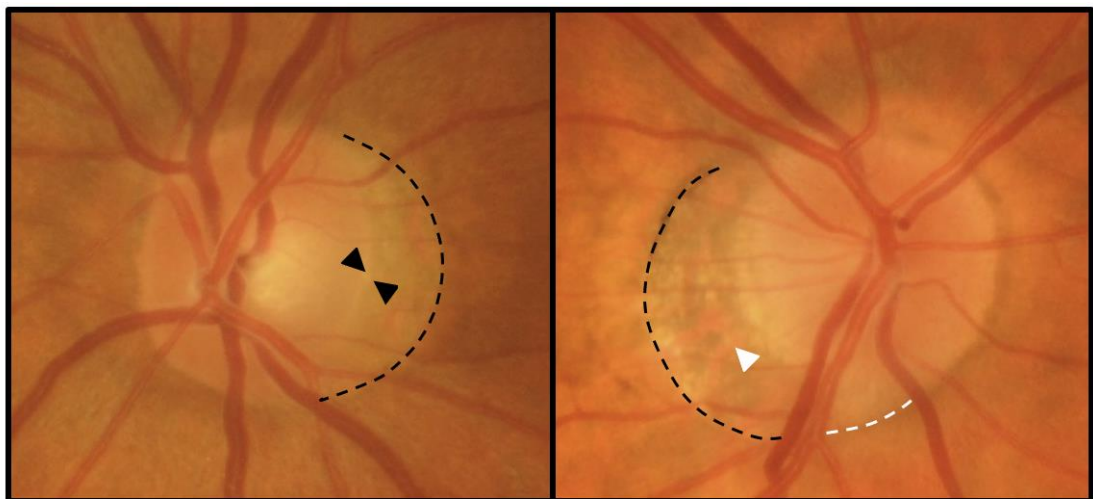


*Figure 3-6 Appearance of beta parapapillary atrophy. Left:* Classic appearance of beta parapapillary atrophy on temporal side of the optic nerve head, with its distal border marked with black stippled lines. The appearance of the beta zone is bright yellowish and have visible choroidal vessels. The two black arrowheads indicate the scleral ring of Elschnig. **Right:** Beta parapapillary atrophy inside stippled lines. The area is yellowish but has darker patches within the zone. Choroidal vessels are visible and marked with the white arrowhead. The white stippled lines indicate a zone of atrophy that did not match the beta- or alpha definition, and therefore was unclassified. As a retinal blood vessel separates this zone from the beta zones identity, the area was evaluated separately and was registered as unclassified parapapillary atrophy.

*Table 3-2 Differentiation of retinal zones.* The table shows the different categories that needed to be identified and differentiated in determination of certain beta parapapillary atrophy. Note that Elschnig’s ring, normal retinal tissue and optic disc are not listed in the table, but needs to be differentiated as well, as mentioned above.

	<b>Beta</b>	<b>Unclassified</b>	<b>Alpha</b>
<b>Appearance</b>	Whitish or bright yellowish area, sometimes blending in with smaller or bigger darker patches within the same area, with transparency to one or several large visible choroidal vessels within parts or the whole beta zone	Neither beta- or alpha parapapillary atrophy or healthy retinal tissue or scleral ring of Elschnig or the optic disc itself	Less transparent, irregularly hyper- and hypo pigmented area, compared with the adjacent borders
<b>Adjacent central border</b>	Scleral ring of Elschnig or the optic disc rim	Scleral ring of Elschnig or the optic disc rim	Beta zone or unclassified zone or scleral ring of Elschnig or the optic disc rim
<b>Adjacent distal border</b>	Alpha zone or normal retinal tissue	Alpha zone or normal retinal tissue	Normal retinal tissue
<b>Appearance of underlying choroidal blood vessels</b>	Exposed, large blood vessels, due to devoid of overlying retinal tissue.  Seen in contrast with underlying sclera.	Either not visible at all, or exposed, large blood vessels, due to devoid or some devoid of overlying retinal tissue.  If visible: Seen in contrast with underlying sclera.	Unexposed large blood vessels, due to some degree of remaining retinal tissue.  Sometimes seen through the retinal tissue if thin retina.
	Less defined in terms of colour and sharpness, than overlying retinal blood vessels. Directional shape often more random curved in opposition to the straighter directional shape of retinal vessels, or radially directed away from the optic disc.		

### 3.5.2.3 *Marking the distal border of beta parapapillary atrophy*

Marking of certain beta parapapillary atrophy and unclassified parapapillary atrophy was made at the distal border of the atrophy, with the pencil tool in Adobe Photoshop Elements. This was done by marking several 6-pixel thick dots centrally and evenly placed along the distal border. A straight line was created between the initial dot and the



next dot, by holding in “shift” button during marking, which connected all dots together, creating a 6-pixel thick line following the curves of the atrophy’s distal border (figure 3-7). As connection of two dots created a straight line in between, each dot was subjectively determined, according to the steepness of the curvature of the distal border. If distal border curvature was straight, the distance between each dot would be longer than if the dots were to follow a steeper curved border that would have been more accurately defined.

The colour of the line was black when it was certain that there was a presence of beta parapapillary atrophy and the distal border was possible to define, according to the definitions of the appearance and the distal border of beta parapapillary atrophy. The colour of the line was green if it was certain beta parapapillary atrophy present, but the distal border was less defined. Unclassified parapapillary atrophy was marked with light blue colour at its distal border. This marking was done regardless of the distal border appearing defined or less defined. Sometimes, a beta parapapillary atrophy could appear within the same zone as unclassified parapapillary atrophy, but then, the identity of the present beta was extended to yield for the whole zone independently of abruption of large retinal arterioles and venules if the identity was the same. If the identity of beta atrophy changed after abruption of a retinal vessel, the area would be evaluated separately (figure 3-6). Any markings had to be affiliated with the optic disc or any visible scleral ring. If neither beta- or unclassified parapapillary atrophy was present and therefore no distal border to mark, no marks were drawn in that image layer in Photoshop Elements.

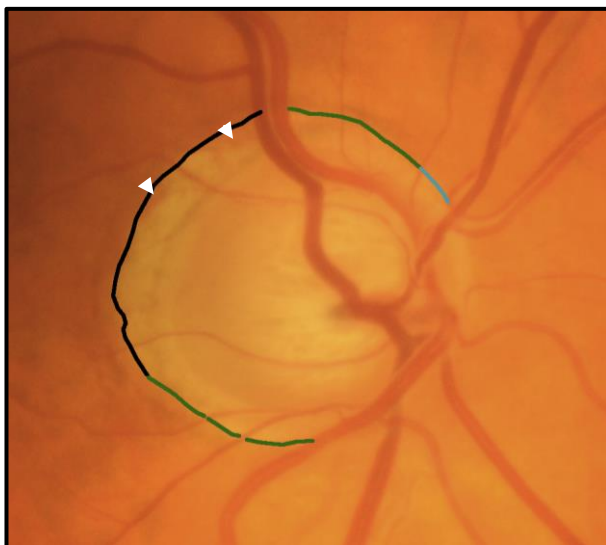


*Figure 3-7 Marking of distal border of parapapillary atrophy.* The parapapillary atrophy adjacent to this optic nerve head was classified as beta with certain border (black line), beta with uncertain border (green line) and unclassified atrophy (light blue line). Choroidal vessels and white/yellowish coloured sclera are visible. The unclassified atrophy is white/yellowish without choroidal vessels and separated from the rest of the “beta-identity” by a retinal blood vessel.

### 3.5.3 Image processing part II: Overlapping fundus- and IR-images

#### 3.5.3.1 *Distal border of beta parapapillary atrophy on SD-OCT*

The IR-images, named as described in figure 3-3, had been marked by the second observer (M.R.) in the image program ImageJ (NATIONAL INSTITUTES of Health, version 1.52K, 2019), as described in detail in Annex 6. Cross-sectional OCT images for right and left eye for the same subjects as described had been analysed in terms of presence of beta parapapillary atrophy and marking of its distal border on IR-image had been done. The markings were done by measuring the distance in pixels from the centre of the optic disc to the ending of atrophy at its distal border on the cross-sectional OCT image, before transferring the measurement to the IR image. The centre of the optic nerve head was defined as the centre of the radial cross overlying the optic nerve head on the IR-image. The radial cross correlated to the anatomic location of the cross-sectional OCT image that had been analysed by the second observer. Beta parapapillary atrophy on SD-OCT was defined as “an area devoid of retinal pigment epithelium, seen as the upper part of the lowermost hyperreflective complex layer, but with intact Bruch’s membrane, seen as the lower part of the lowermost hyperreflective complex or as a single hyperreflective lowermost layer (when retinal pigment epithelium is lost) (Dai et al., 2013; Hayashi et al., 2012; Kim et al., 2013; Lee et al., 2010; Miki et al., 2017; Miki et al., 2019; Vianna et al., 2016; Zhang et al., 2018)” (Annex 6). The distal border of the beta parapapillary atrophy on SD-OCT was defined as the exact point where denuded Bruch’s membrane bordered with overlying retinal pigment epithelium.

A yellow line was drawn from the centre of the cross (centre of the optic nerve head) along the 15-degree separated radial lines on the IR-images that had beta parapapillary atrophy, to the distal border of the beta atrophy. For this study, the exact location where the yellow line stopped, was determined as the OCT-defined distal border of the beta parapapillary atrophy (+/- 0.5 pixels). If no beta parapapillary atrophy was present in a

section, no marking along the line was done. If the distal border of the atrophy was uncertain, a blue oblique line was drawn across the radial scans' line. If the distal border of atrophy was not visible, it was excluded in that section, and a red oblique line was drawn across the radial scans' line. If gamma parapapillary atrophy was present when beta was not present, it was drawn an orange line along the scans' line in that section. Any other colour drawn along the lines of the radial cross on the IR-image was not relevant for this study (Annex 6). The baseline colour of the radial cross on IR-images was green, but one of the sections could sometimes be turquoise or red. An example of a marked IR-image is seen in figure 3-8. The purpose of having a second observer analysing OCT-images was to blind the main observer in the process of analysing fundus photos and overlapping images.

#### *3.5.3.2 Overlapping fundus photographs and IR-Images*

Fundus photographs and their layers was opened in Adobe Photoshop Elements, with only the "Quality layer" visible. Thereafter, the marked IR-image was overlaid the fundus image in a separate layer and was fitted according to landmarks like blood vessels by increasing and adjusting the size and rotating the IR-image, along with frequently changing the opacity of the overlying layer, to see if the images would match (figure 3-8). When overlapping was done, the file was stored by overwriting existing image file, and name the file according to figure 3-1 in the last step of image storage. The marked IR-images served as blueprints for the fundus photographs. The overlapped IR-image added the definition of the radial sections to the fundus photo, making registration of beta on fundus photographs and distal border possible with high certainty.

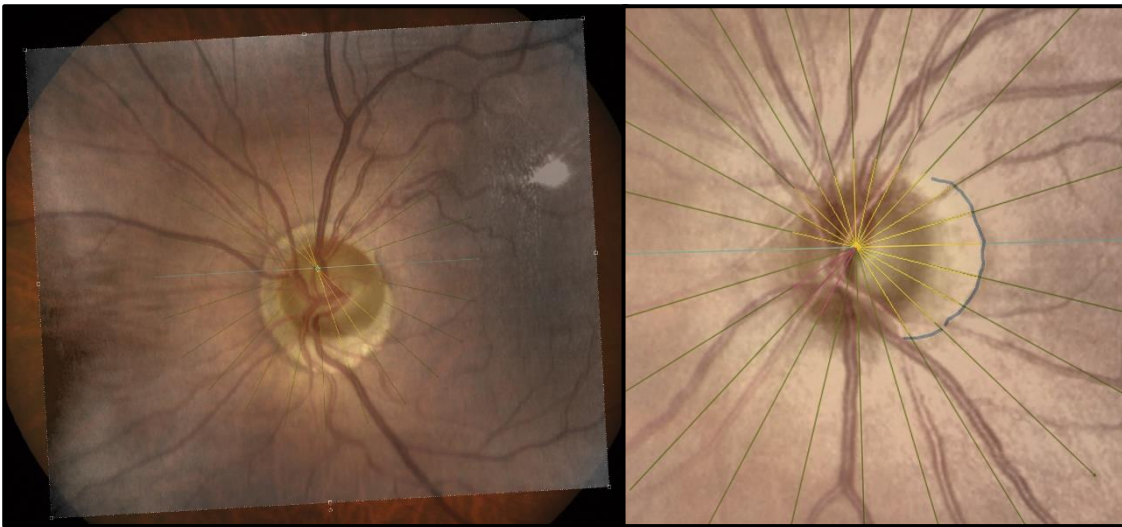


*Figure 3-8 Markings of OCT-defined border on a transparent IR-image overlaid on underlying fundus image. **Left:** The image shows the overlapping procedure, where the blood vessels and landmarks of both images are aligned. Any marking of parpapillary atrophy of the fundus image was not visible at this stage in the analyses, as it was important that there was no confirmation bias in comparing fundus photo with SD-OCT. **Right:** An example of an IR-image with reduced opacity to compare the visible marking on fundus photo.*

### *3.5.3.3 Registration of presence of beta parpapillary atrophy and its distal border*

All the data was registered by hand in a registration form (Annex 5). The presence of fundus photo-defined beta parpapillary atrophy was registered based on the colour of the presence and colour of marked line on the fundus photo. The categories registered was “No atrophy”, “Beta (with certain border)”, “Beta with uncertain border”, “Unclassified atrophy” and “Missing data” for each section. The same registration was done for total presence in right, left and both eyes, but beta atrophy was registered regardless of uncertain border, and unclassified atrophy was registered only when beta was not present.

The distal border of beta parpapillary atrophy was registered based on OCT-defined borders relative to the location of the fundus photo-defined borders. Opacity was changed of the overlying IR-image, to see the markings of both images. Registration was done for: “No beta present”, “Overlapping distal border”, “OCT-defined border located on the inside”, “OCT-defined border located on the outside”, “Unverified” and “Missing data” for each section. An overview of when to choose the different categories is shown in table 3-3.

The presence of OCT-defined beta parapapillary atrophy was registered by the second observer (M.R.), and the dataset was given to main observer via encrypted USB. The frequency of beta parapapillary atrophy for right, left and both eyes, along with distribution of frequencies in 15-degree separated sections around optic nerve head was found as described in chapter 3.6, by excluding eyes from the OCT data set to match the fundus photo data set.

*Table 3-3 Categories for registration of Distal border of beta parapapillary atrophy*

<b>Categories for distal border of beta PPA relative to fundus-defined border</b>	<b>Descriptions of when categories for distal border of beta PPA should be registered</b>
<b>No beta present</b>	- <i>No presence</i> of beta PPA on IR-image and fundus image
<b>Overlapping distal border</b>	- Beta PPA present and marked on both IR-image (yellow line) and fundus image (black and green line), and both markings <i>overlap</i> with at least one pixel, or by touching pixel to pixel at 100% magnification.
<b>OCT-defined border located on the inside</b>	- Beta PPA present and marked on IR-image (yellow line) and on fundus image (black and/or green line), but OCT-defined border is located on the <i>inside</i> of the fundus photo-defined border.
<b>OCT-defined border located on the outside</b>	- Beta PPA present and marked on IR-image (yellow line) and on fundus image (black and/or green line), but OCT-defined border is located on the <i>outside</i> of the fundus photo-defined border.
<b>Unverified</b>	- Beta PPA present and marked (yellow line) <i>only</i> on IR-image, (but not on fundus image). - Beta PPA present and marked (black and/or green line) <i>only</i> on fundus image (but not on IR-image). - <i>Unclassified</i> PPA (light blue line) marked on photo. - <i>Uncertain</i> marking (blue oblique line) on IR-image.
<b>Missing data</b>	- Missing data on <i>both</i> IR-image and fundus image. - Missing data on <i>either</i> IR-image or fundus image.

PPA= parapapillary atrophy

### **3.6 Reproducibility and repeatability**

After analysing the images in Image processing part I (chapter 3.4) regarding image quality and presence and marking of beta parapapillary atrophy, the process was overlooked a second time by the main observer to be sure of the definitions that was done. The definitions were looked through at this point, and in some cases adjusted, to minimize any possible risk of subjective interpretations in favour over a standardized definition. A consensus meeting with a trained observer/supervisor (P.O.L) was held regarding 20 images that was uncertain to define. Another 20 randomly chosen images that was certainly defined by main observer was also discussed and a consensus was

reached. The overlapping procedure was done for all images, and when registration was done, the overlapping was controlled once more. Any adjustments were then done before registration in the registration form. The OCT-images had been quality assured by second observer. The excel sheet with the plotted values from the registration forms was quality assured before statistic analyses.

### **3.7 Statistics**

The complete data set was transferred from Excel to the statistical program SPSS (IBM SPSS Statistics, version 25, 2017). Descriptive statistics was used for the statistic analyses. For demographics, frequency was used for categorical nominal variables, and mean with standard deviation (SD) was used for continuous variables. For the rest of the analysis's frequency was used for both categorical nominal variables (presence of beta in eyes and distribution of frequencies around optic disc and distal border of beta in fundus photo) and for ordinal variables (image quality). For frequency and distribution of frequencies of beta parapapillary atrophy on SD-OCT, the relevant data set in SPSS was given to the main observer by a second observer (M.R.), and the same statistical analyses were done as described above for fundus photo. Significance tests was done for frequency of presence of beta parapapillary atrophy and total image quality by comparing right and left eye for fundus photo with a significance level of  $p < 0.05$ . For frequency of presence of beta, McNemar test was used. For frequency of image quality, Wilcoxon signed rank test was used. The frequency results for presence of beta parapapillary atrophy and its distal border on fundus photo and OCT were plotted in Excel. A 95% confidence interval (CI) was calculated only for prevalence in right, left and both eyes, and for distribution of frequencies on fundus photo and SD-OCT. Frequencies and CI for both image modalities were plotted in a polar diagram for right and left eye with a scale numerated from 0 to 345 degrees with 15-degree separation around a schematic optic nerve head, according to the same scan pattern on IR-images and the same numerating of scan-lines as seen in figure 3-2. The scale was mirrored for right eye both in tables in excel and in the polar diagram, so the numbers would correlate to the same anatomical areas when referring to the numbers on the scale. For the distribution of frequencies of the distal border of beta parapapillary atrophy, a column chart was made to illustrate the distribution of percentage of location of OCT-defined and fundus photo-defined borders, unverified borders and no presence of atrophy. The distribution of percentage on the y-axis was added to 100 percent, and all

the sections from 0-345 in the scan pattern was distributed on the x-axis, and mirrored for right eye, as for the same reason as described above. CI was calculated in Excel only for the overlapping border.

### **3.8 Ethics**

All investigations in the DVOH- and sub-study adhered to the tenets of the Declaration of Helsinki and was approved by the Regional Committee for Medical Research Ethics for the Southern Norway Regional Health Authority (REK). There were no obligations for the optometric shops or the people receiving information about the study.

Information was given written and oral, before a consent form was signed by the subjects, with possibility of withdrawal at any time without any given reason. The optometric examination duration was 3-3.5 hours overall, but the investigation relevant for this sub-study was estimated to maximum 45 minutes per subject. Re-scheduling for completion of examination was optional if needed, but this was rarely the case, as there were room for frequently breaks, and one break of 20 minutes was given to all subjects, as this time was needed for the topical diagnostic medication to work. Each test had relatively short duration. All the tests conducted are accepted as safe within the field of optometry and the Tropicamide that was used is approved by the Food and Drug Administration (FDA), and has only mild ocular discomfort at insertion. Information was given to the subjects about potential normal and more severe but rare side effects (Felleskatalogen). The instrumentation used had no risk of hazardous health outcome. The Kowa Nonmydriatic retinal camera had a flash of light from a xenon lamp, and the Cirrus HD-OCT had a strongly signalled fixation point, in which both could give temporarily after image. The Cirrus HD-OCT has a laser that is classified as Laser Class 1, which means that there is no risk of injury for the subject (Norwegian electrotechnical publication, 2014).

All the observers that collected data from the examination was optometrists regulated by the Norwegian law for health care professionals, and the subjects was protected by the Norwegian law for Patient Rights (Helsepersonelloven, 1999; Pasient- og brukerrettighetsloven, 1999). Each observer had responsibility of electronic documentation in journal systems, according to Norwegian law for health care professionals (Helsepersonelloven, 1999, § 39), and, if necessary, follow-up or referrals of the subjects to general practitioner or ophthalmologist was done. Duty of confidentiality applied to all observers (Helsepersonelloven, 1999, § 21). An ID-key

was made for handling of data post-examination, as described in chapter 3.5.1 to ensure anonymization of the subjects. As further described in chapter 3.5.1, the ID-key was stored safely online on Figshare (figure 3-1), with limited access, and the password and username for access will be deleted at latest 31<sup>st</sup> of December 2019. The same date is deadline for transferring images from the image analyses of this study to the main investigator of DVOH from the locally stored password-protected and limited accessed computer by main observer.



## 4 Results

The study included overall 68 out of 70 subjects, with a total of 135 eyes. Exclusion was done due to missing fundus photographs. Inclusion and reason for inclusion for the different results are shown table 4-1.

*Table 4-1 Exclusion and inclusion in the statistical analyses.* The table shows how many subjects eyes/images that was excluded, and reasons why in each step of the analyses.

<b>Eyes/Images</b>	<b>Right</b>	<b>Left</b>
<b>Included to study/ analyses of image quality</b>	<b><math>N=70 - 2 = \underline{68}</math></b>	<b><math>N=70 - 3 = \underline{67}</math></b>
	Exclusion due to missing fundus photo	
<b>Included for analyses of frequency of beta on fundus photo and analyses of distal border of beta on fundus photo and OCT</b>	<b><math>N=68 - 2^* - 2^\# = \underline{64}</math></b>	<b><math>N=67 - 2^* - 2^\# = \underline{63}</math></b>
	* Exclusion due to total image quality = 1 # Exclusion due to excessive decentration of radial scan outside optic nerve head on IR-image	
<b>Included to study/analyses of frequency of beta on OCT and comparison of frequencies between fundus photo and OCT</b>	<b><math>N=70 - 6 = \underline{64}</math></b>	<b><math>N=70 - 7 = \underline{63}</math></b>
	Exclusion due to the same reasons as described above	

### 4.1 Demographics

Demographical results regarding gender, age and refractive error is listed in table 4-2. For ocular disease, 10 (14.7%) subjects had diabetic retinopathy, no subjects had age-related macular degeneration (AMD) and 1 (1.5%) subject had another kind of retinopathy. Glaucoma was present in 3 (4.4%) subjects and cataract was present in 18 (26.5%) subjects.

Table 4-2 Demographical results of gender, age and refractive error.

N=68	
n (%)	
Males	35 (51.5%)
Females	33 (48.5%)
Mean $\pm$ SD (range)	
Age	66.72 $\pm$ 9.419 years (43, 81)
Subjective sphere RE	-0.0551 $\pm$ 2.81582 D (-11.00, +8.25)
Subjective cylinder RE	-0.8952 $\pm$ 0.61329 DC (-3.50, -0.25)
Subjective sphere LE	-0.1765 $\pm$ 2.64894 D (-9.50, +7.00)
Subjective cylinder LE	-0.9280 $\pm$ 0.69489 DC (-4.50, -0.25)

D= diopter, DC= dioptic cylinder

## 4.2 Image quality of fundus photographs

135 eyes with belonging 68 fundus photographs for right eye and 67 fundus photographs for left eye were included for evaluation of image quality. Four photographs were graded 1 “Poor Quality” and was excluded from the rest of the analyses. Results for image quality of all 135 fundus photographs are shown in table 4-3. There was an insignificant difference between left and right eye ( $p= 0.564$ ).

Table 4-3 Frequencies of different gradings of sharpness, exposure and total image quality for right and left eye.

	Eye	Grade 1 Poor quality n/N (%)	Grade 2 Intermediate quality n/N (%)	Grade 3 Good quality n/N (%)
Sharpness	RE	2/68 (2.9)	45/68 (66.2)	21/68 (30.9)
	LE	1/67 (1.5)	43/67 (64.2)	23/67 (34.3)
Exposure	RE	0/68 (0)	13/68 (19.1)	55/68 (80.9)
	LE	1/67 (1.5)	13/67 (19.4)	53/67 (79.1)
Total Quality	RE	2/68 (2.9)	47/68 (69.1)	19/68 (27.9)
	LE	2/67 (3.0)	43/67 (64.2)	22/67 (32.8)
Total quality of all images		4/135 (3.0)	90/135 (66.7)	41/135 (30.4)

### **4.3 Frequency of beta parapapillary atrophy by means of fundus photography**

64 images for right eye, 63 images for left eye and 60 images for both eyes were included, all to which had a total image quality of grade 2 or 3.

Frequency of beta parapapillary atrophy for right eyes was 15 (23.4%, CI: 13.0, 33.8).

For left eyes the frequency of beta parapapillary atrophy was 17 (27.0%, CI: 16.0, 38.0).

There was an insignificant difference between right and left eyes ( $p= 0.550$ ).

Frequency of beta parapapillary atrophy in both eyes was 13 (21.7%, CI: 11.3, 32.1).

When beta parapapillary atrophy was not present, frequency of unclassified parapapillary atrophy was 10 for right (15.6%) and left eye (15.9%). Frequency for both eyes was 3 (5.0%).

#### **4.3.1 Frequency of beta parapapillary atrophy with total image quality grade 2 and 3 done separately**

Two separated tests for prevalence of beta parapapillary atrophy only in eyes with total image quality grade 2 and eyes only with total image quality grade 3 was done. With total image quality grade 2, 45 eyes were included for right eye and 42 eyes were included for left eye.

Frequency of beta parapapillary atrophy in right eye with total image quality grade 2 was 11 (24.4%). For left eye the frequency was 13 (31.0%). With total image quality grade 3, 19 eyes were included for right eye and 21 eyes were included for left eye. Frequency of beta parapapillary atrophy in right eye with total image quality grade 3 was 4 (21.1%). For left eye the frequency was 4 (19.0%).

### **4.4 Distribution of frequencies of beta parapapillary atrophy around the optic nerve head by means of fundus photography**

64 right eyes and 63 left eyes was included for distribution of frequencies of beta parapapillary atrophy by means of fundus photography. Distribution of frequencies of

beta parapapillary atrophy around the optic nerve head is graphically illustrated in chart 4-1 and listed in table 4-4 for right and left eye with a 95% confidence interval. The distribution of frequencies of beta parapapillary atrophy with a certain distal border, beta atrophy with an uncertain distal border, no beta parapapillary atrophy and unclassified atrophy for right and left eye are listed in a table in Annex 7.

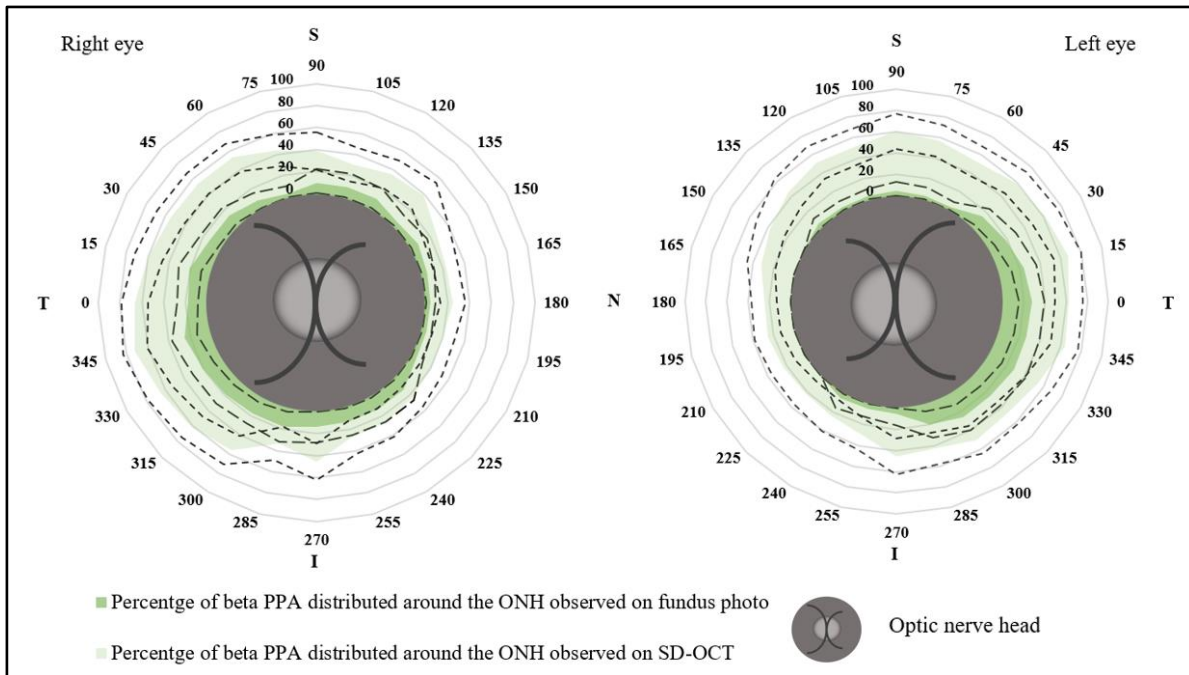


*Chart 4-1 Distribution of frequencies of beta parapapillary atrophy surrounding the optic nerve head on fundus photo and SD-OCT in right and left eye. The charts illustrate the distribution for frequency of beta parapapillary atrophy, around the optic nerve head which is indicated in the middle of the charts, with presentation of prevalence in each 15-degree separated sections around the nerve head for right and left eye. The scale for percentage ranges from 0% to 100% and starts as indicated at the border of the schematic optic nerve head. Letters T, S, N and I indicates temporal, superior, nasal and inferior location around the optic nerve head. The dark green colour indicates the distribution of frequencies of beta atrophy on fundus photo and the bright green colour indicates distribution of frequencies of beta on SD-OCT, with belonging 95% confidence intervals for both image modalities. Long stippled lines indicate 95% confidence intervals for percentage of beta atrophy on fundus photo and short stippled lines illustrates the same for SD-OCT. Note that the coloured areas must not be mistaken with areal of atrophies. Values between the degrees were extrapolated.*

Table 4-4 Distribution of frequencies of beta parapapillary atrophy around the optic nerve head in right and left eye based on fundus photo.

Presence of beta PPA					
Degree/eye		n/N (%) [CI: 0.0, 0.0]	Degree/eye		n/N (%) [CI: 0.0, 0.0]
0	RE	11/60 (18.3) [8.5, 28.1]	180	RE	2/52 (3.8) [0.0, 9.0]
	LE	14/51 (27.5) [15.2, 39.8]		LE	0/45 (0) [0.0, 0.0]
15	RE	11/54 (20.4) [9.7, 31.1]	195	RE	2/52 (3.8) [0.0, 9.0]
	LE	12/49 (24.5) [12.5, 36.5]		LE	0/44 (0) [0.0, 0.0]
30	RE	6/45 (13.3) [3.4, 23.2]	210	RE	2/42 (4.8) [0.0, 11.3]
	LE	8/43 (18.6) [7.0, 30.2]		LE	0/36 (0) [0.0, 0.0]
45	RE	6/46 (13.0) [3.3, 23.2]	225	RE	3/24 (12.5) [0.7, 25.7]
	LE	6/42 (14.0) [3.6, 24.4]		LE	0/19 (0) [0.0, 0.0]
60	RE	3/40 (7.5) [0.0, 15.7]	240	RE	3/24 (12.5) [0.7, 25.7]
	LE	1/34 (2.9) [0.0, 8.5]		LE	1/19 (5.3) [0.0, 15.4]
75	RE	1/30 (3.3) [0.0, 9.7]	255	RE	3/24 (12.5) [0.0, 25.7]
	LE	1/26 (3.8) [0.0, 11.1]		LE	1/24 (4.2) [0.0, 12.2]
90	RE	2/21 (9.6) [0.0, 22.2]	270	RE	3/22 (13.6) [0.0, 28.0]
	LE	1/22 (4.5) [0.0, 13.2]		LE	1/18 (5.6) [0.0, 16.2]
105	RE	2/21 (9.6) [0.0, 22.2]	285	RE	5/28 (17.9) [0.0, 32.1]
	LE	1/29 (3.4) [0.0, 10.0]		LE	7/36 (19.5) [6.6, 32.4]
120	RE	3/31 (9.7) [0.0, 20.1]	300	RE	7/42 (16.7) [0.0, 28.0]
	LE	1/31 (3.2) [0.0, 9.4]		LE	10/39 (25.6) [11.9, 39.3]
135	RE	1/22 (4.5) [0.0, 13.2]	315	RE	8/43 (18.6) [7.0, 30.2]
	LE	1/26 (3.8) [0.0, 11.1]		LE	11/44 (25.0) [12.2, 37.8]
150	RE	2/28 (7.2) [0.0, 16.8]	330	RE	10/50 (20.0) [8.9, 31.1]
	LE	0/20 (0) [0.0, 0.0]		LE	12/43 (27.9) [14.5, 41.3]
165	RE	2/40 (5.0) [0.0, 11.8]	345	RE	13/52 (25.0) [13.2, 36.8]
	LE	0/44 (0) [0.0, 0.0]		LE	13/48 (27.1) [14.5, 39.7]

PPA= parapapillary atrophy

## 4.5 Distribution of frequencies of beta parapapillary atrophy around the optic nerve head by means of fundus photography and SD-OCT

### 4.5.1 Frequency of beta parapapillary atrophy by means of SD-OCT

64 right eyes and 63 left eyes was included. Frequency of beta parapapillary atrophy defined on SD-OCT for right eyes was 51 (79.7%, CI: 69.8, 89.6). For left eyes the

frequency of parapapillary atrophy was 41 (65.1%, 53.3, 76.9). Frequency of beta parapapillary atrophy in both eyes was 36 (60.0%, 47.6, 72.4).

#### 4.5.2 Distribution of frequencies of beta parapapillary atrophy around the optic nerve head by means of SD-OCT

64 right eyes and 63 left eyes was included. Distribution of frequencies of beta parapapillary atrophy observed in radial segments around the optic nerve head by means of SD-OCT is listed in table 4-5.

Chart 4-1 gives an illustration of the distribution of frequencies of beta parapapillary atrophy identified on both SD-OCT and fundus photography.

*Table 4-5 Distribution of frequencies of beta parapapillary atrophy around the optic nerve head in right and left eye based on SD-OCT.*

Presence of beta PPA					
Degree/eye		n/N (%) [CI: 0.0, 0.0]	Degree/eye		n/N (%) [CI: 0.0, 0.0]
<b>0</b>	<b>RE</b>	<b>40/60 (66.7)</b> [54.8, 78.6]	<b>180</b>	<b>RE</b>	<b>14/57 (24.6)</b> [13.5, 35.7]
	<b>LE</b>	<b>32/51 (62.7)</b> [49.4, 76.0]		<b>LE</b>	<b>12/48 (25.0)</b> [12.8, 37.3]
<b>15</b>	<b>RE</b>	<b>34/57 (59.6)</b> [46.9, 72.3]	<b>195</b>	<b>RE</b>	<b>11/55 (20.0)</b> [9.4, 30.6]
	<b>LE</b>	<b>33/49 (67.3)</b> [54.2, 80.4]		<b>LE</b>	<b>12/46 (26.1)</b> [13.4, 38.8]
<b>30</b>	<b>RE</b>	<b>28/51 (54.9)</b> [41.2, 68.6]	<b>210</b>	<b>RE</b>	<b>10/48 (20.8)</b> [9.3, 32.3]
	<b>LE</b>	<b>29/47 (61.7)</b> [47.8, 75.6]		<b>LE</b>	<b>9/39 (23.1)</b> [9.9, 36.3]
<b>45</b>	<b>RE</b>	<b>27/50 (54.0)</b> [40.2, 67.8]	<b>225</b>	<b>RE</b>	<b>9/39 (23.1)</b> [9.9, 36.3]
	<b>LE</b>	<b>27/46 (58.7)</b> [44.5, 72.9]		<b>LE</b>	<b>6/28 (21.4)</b> [6.2, 36.6]
<b>60</b>	<b>RE</b>	<b>25/47 (53.2)</b> [38.9, 67.5]	<b>240</b>	<b>RE</b>	<b>9/34 (26.5)</b> [11.7, 41.3]
	<b>LE</b>	<b>22/42 (52.4)</b> [37.3, 67.5]		<b>LE</b>	<b>6/25 (24.0)</b> [7.3, 40.7]
<b>75</b>	<b>RE</b>	<b>18/41 (43.9)</b> [28.7, 59.1]	<b>255</b>	<b>RE</b>	<b>9/33 (27.3)</b> [12.1, 42.5]
	<b>LE</b>	<b>24/42 (57.1)</b> [42.1, 72.1]		<b>LE</b>	<b>11/38 (28.9)</b> [14.5, 43.3]
<b>90</b>	<b>RE</b>	<b>12/31 (38.7)</b> [21.6, 55.8]	<b>270</b>	<b>RE</b>	<b>15/33 (45.5)</b> [28.5, 62.5]
	<b>LE</b>	<b>20/33 (60.6)</b> [43.9, 77.3]		<b>LE</b>	<b>15/33 (45.5)</b> [28.5, 62.5]
<b>105</b>	<b>RE</b>	<b>10/33 (30.3)</b> [14.6, 46.0]	<b>285</b>	<b>RE</b>	<b>12/36 (33.3)</b> [17.9, 48.7]
	<b>LE</b>	<b>18/35 (51.4)</b> [34.8, 68.0]		<b>LE</b>	<b>18/42 (42.9)</b> [27.9, 57.9]
<b>120</b>	<b>RE</b>	<b>15/42 (35.7)</b> [21.2, 50.2]	<b>300</b>	<b>RE</b>	<b>24/43 (55.8)</b> [41.0, 70.6]
	<b>LE</b>	<b>17/33 (51.5)</b> [34.4, 68.6]		<b>LE</b>	<b>22/44 (50.0)</b> [35.2, 64.8]
<b>135</b>	<b>RE</b>	<b>14/36 (38.9)</b> [23.0, 54.8]	<b>315</b>	<b>RE</b>	<b>30/49 (61.2)</b> [47.6, 74.8]
	<b>LE</b>	<b>14/31 (45.2)</b> [27.7, 62.7]		<b>LE</b>	<b>23/48 (47.9)</b> [33.8, 62.0]
<b>150</b>	<b>RE</b>	<b>11/42 (26.2)</b> [12.9, 39.5]	<b>330</b>	<b>RE</b>	<b>34/52 (65.4)</b> [52.5, 78.3]
	<b>LE</b>	<b>15/40 (37.5)</b> [22.5, 52.5]		<b>LE</b>	<b>26/48 (54.2)</b> [40.1, 68.3]
<b>165</b>	<b>RE</b>	<b>12/53 (22.6)</b> [11.3, 33.7]	<b>345</b>	<b>RE</b>	<b>42/58 (72.4)</b> [60.9, 83.9]
	<b>LE</b>	<b>15/46 (32.6)</b> [19.1, 46.1]		<b>LE</b>	<b>32/50 (64.0)</b> [50.7, 77.3]

PPA= parapapillary atrophy

## 4.6 Distribution of frequencies of distal border of beta parapapillary atrophy by means of fundus photo and SD-OCT

64 right eyes and 63 left eyes was included for distribution of frequencies of distal border of beta parapapillary atrophy by means of fundus photo and SD-OCT.

Distribution is shown for right and left eye in table 4-6, with belonging 95% confidence interval for overlapping distal borders, and in chart 4-2 and chart 4-3 for right and left eye, respectively.

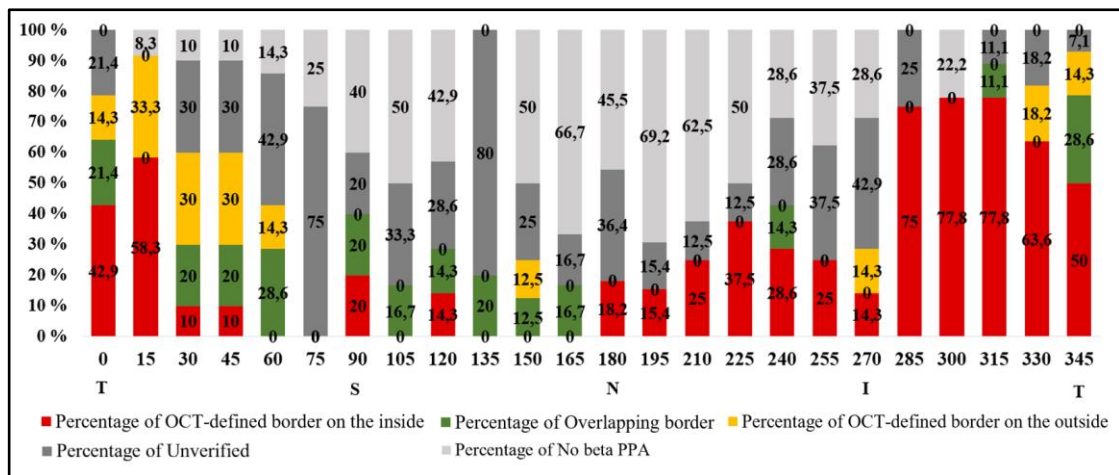


Chart 4-2 Distribution of frequencies of distal border of beta parapapillary in right eye.

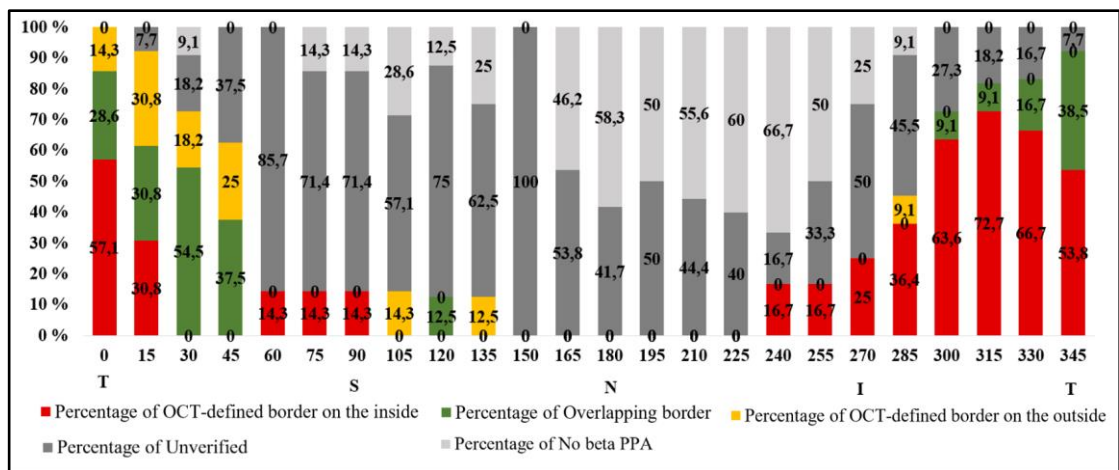


Chart 4-3 Distribution of frequencies of distal border of beta parapapillary in left eye.

Chart 4-2 (top) and chart 4-3 (bottom): The charts shows the distribution of frequencies of location of distal border of beta parapapillary atrophy for each 15-degree separated sections around the optic nerve head. Letters T, S, N and I indicates temporal, superior, nasal and inferior location around the optic nerve head, in addition to the sections given

in degree along the x-axis. The y-axis ranges from 0-100% and shows the total distribution of percentage of categories for distal border. The location of the distal borders is defined according to the fundus photo-defined distal border.

*Table 4-6 Distribution of frequencies of distal border of beta parapapillary atrophy in right and left eyes.* The table shows the different categories for distal border of beta parapapillary atrophy. The location of the distal borders is defined according to the fundus photo-defined distal border. 95% confidence interval is listed for the overlapping distal borders.

Degree/eye		OCT-defined border on the inside	Overlapping border n/N (%) [CI: 0.0, 0.0]	OCT-defined border on the outside	Unverified border	No presence of beta PPA
0	RE	6/14 (42.9)	3/14 (21.4) [0.1, 42.9]	2/14 (14.3)	3/14 (21.4)	0/14 (0)
	LE	8/14 (57.1)	4/14 (28.6) [4.9, 52.3]	2/14 (14.3)	0/14 (0)	0/14 (0)
15	RE	7/12 (58.3)	0/12 (0) [0.0, 0.0]	4/12 (33.3)	0/12 (0)	1/12 (8.3)
	LE	4/13 (30.8)	4/13 (30.8) [5.7, 55.9]	4/13 (30.8)	1/4 (7.7)	0/13 (0)
30	RE	1/10 (10.0)	2/10 (20.0) [0.0, 44.8]	3/10 (30.0)	3/10 (30.0)	1/10 (10.0)
	LE	0/11 (0)	6/11 (54.5) [25.1, 84]	2/11 (18.2)	2/11 (18.2)	1/11 (9.1)
45	RE	1/10 (10.0)	2/10 (20) [0.0, 44.8]	3/10 (30.0)	3/10 (30.0)	1/10 (10.0)
	LE	0/8 (0)	3/8 (37.5) [4.0, 71.0]	2/8 (25.0)	3/8 (37.5)	0/8 (0)
60	RE	0/7 (0)	2/7 (28.6) [0.0, 62.1]	1/7 (14.3)	3/7 (42.9)	1/7 (14.3)
	LE	1/7 (14.3)	0/7 (0) [0.0, 0.0]	0/7 (0)	6/7 (85.7)	0/7 (0)
75	RE	0/4 (0)	0/4 (0) [0.0, 0.0]	0/4 (0)	3/4 (75.0)	1/4 (25.0)
	LE	1/5 (14.3)	0/7 (0) [0.0, 0.0]	0/7 (0)	5/7 (71.4)	1/5 (14.3)
90	RE	1/5 (20.0)	1/5 (20.0) [0.0, 55.1]	0/5 (0)	1/5 (20.0)	2/5 (40.0)
	LE	1/7 (14.3)	0/7 (0) [0.0, 0.0]	0/7 (0)	5/7 (71.4)	1/7 (14.3)
105	RE	0/6 (0)	1/6 (16.7) [13.1, 46.5]	0/6 (0)	2/6 (33.3)	3/6 (50.0)
	LE	0/7 (0)	0/7 (0) [0.0, 0.0]	1/7 (14.3)	4/7 (57.1)	2/7 (28.6)
120	RE	1/7 (14.3)	1/7 (14.3) [0.0, 40.2]	0/7 (0)	2/7 (28.6)	3/7 (42.9)
	LE	0/8 (0)	1/8 (12.5) [0.0, 35.4]	0/8 (0)	6/8 (75.0)	1/8 (12.5)
135	RE	0/5 (0)	1/5 (20.0) [0.0, 55.1]	0/5 (0)	4/5 (80.0)	0/5 (0)
	LE	0/8 (0)	0/8 (0) [0.0, 0.0]	1/8 (12.5)	5/8 (62.5)	2/8 (25.0)
150	RE	0/8 (0)	1/8 (12.5) [0.0, 35.4]	1/8 (12.5)	2/8 (25.0)	4/8 (50.0)
	LE	0/4 (0)	0/4 (0) [0.0, 0.0]	0/4 (0)	4/4 (100)	0/4 (0)
165	RE	0/12 (0)	2/12 (16.7) [0.0, 37.8]	0/12 (0)	2/12 (16.7)	8/12 (66.7)
	LE	0/13 (0)	0/13 (0) [0.0, 0.0]	0/13 (0)	7/13 (53.8)	6/13 (46.2)
180	RE	2/11 (18.2)	0/11 (0) [0.0, 0.0]	0/11 (0)	4/11 (36.4)	5/11 (45.5)
	LE	0/12 (0)	0/12 (0) [0.0, 0.0]	0/12 (0)	5/12 (41.7)	7/12 (58.3)
195	RE	2/13 (15.4)	0/13 (0) [0.0, 0.0]	0/13 (0)	2/13 (15.4)	9/13 (69.2)
	LE	0/14 (0)	0/14 (0) [0.0, 0.0]	0/14 (0)	7/14 (50.0)	7/14 (50.0)
210	RE	2/8 (25.0)	0/8 (0) [0.0, 0.0]	0/8 (0)	1/8 (12.5)	5/8 (62.5)
	LE	0/9 (0)	0/9 (0) [0.0, 0.0]	0/9 (0)	4/9 (44.4)	5/9 (55.6)
225	RE	3/8 (37.5)	0/8 (0) [0.0, 0.0]	0/8 (0)	1/8 (12.5)	4/8 (50.0)
	LE	0/5 (0)	0/5 (0) [0.0, 0.0]	0/5 (0)	2/5 (40)	3/5 (60)
240	RE	2/7 (28.6)	1/7 (14.3) [0.0, 40.2]	0/7 (0)	2/7 (28.6)	2/7 (28.6)
	LE	1/6 (16.7)	0/6 (0) [0.0, 0.0]	0/6 (0)	1/6 (16.7)	4/6 (66.7)



255	RE	2/8 (25.0)	0/8 (0) [0.0, 0.0]	0/8 (0)	3/8 (37.5)	3/8 (37.5)
	LE	1/6 (16.7)	0/6 (0) [0.0, 0.0]	0/6 (0)	2/6 (33.3)	3/6 (50.0)
270	RE	1/7 (14.3)	0/7 (0) [0.0, 0.0]	1/7 (14.3)	3/7 (42.9)	2/7 (28.6)
	LE	1/4 (25.0)	0/4 (0) [0.0, 0.0]	0/4 (0)	2/4 (50.0)	1/4 (25.0)
285	RE	3/4 (75.0)	0/4 (0) [0.0, 0.0]	0/4 (0)	1/4 (25.0)	0/4 (0)
	LE	4/11 (36.4)	0/11 (0) [0.0, 0.0]	1/11 (9.1)	5/11 (45.5)	1/11 (9.1)
300	RE	7/9 (77.8)	0/9 (0) [0.0, 0.0]	0/9 (0)	0/9 (0)	2/9 (22.2)
	LE	7/11 (63.6)	1/11 (9.1) [0.0, 26.1]	0/11 (0)	3/11 (27.3)	0/11 (0)
315	RE	7/9 (77.8)	1/9 (11.1) [0.0, 31.6]	0/9 (0)	1/9 (11.1)	0/9 (0)
	LE	8/11 (72.7)	1/9 (11.1) [0.0, 31.6]	0/11 (0)	2/11 (18.2)	0/11 (0)
330	RE	7/11 (63.6)	0/11 (0) [0.0, 0.0]	2/11 (18.2)	2/11 (18.2)	0/11 (0)
	LE	8/12 (66.7)	2/12 (16.7) [0.0, 37.8]	0/12 (0)	2/12 (16.7)	0/12 (0)
345	RE	7/14 (50.0)	4/14 (28.6) [4.9, 52.3]	2/14 (14.3)	1/14 (7.1)	0/14 (0)
	LE	7/13 (53.8)	5/13 (38.5) [12.0, 65.0]	0/13 (0)	1/13 (7.7)	0/13 (0)



## **5 Discussion**

The purpose of the study was to investigate the prevalence and distribution of frequencies of beta parapapillary atrophy and its distal border around the optic nerve head identified by the means of colour fundus photographs and SD-OCT.

### **5.1 Frequency of beta parapapillary atrophy by means of fundus photography**

Prevalence of beta parapapillary atrophy in this study was 23.4% for right eyes and 27.0% for left eyes. There was an insignificant difference between the eyes. Compared with normal population-based studies on prevalence of beta parapapillary atrophy using fundus photography, the results in the current study was slightly higher. The mentioned studies had prevalence from 11.4% to 19.9% in one or both eyes (Jonas et al., 1989; Jonas et al., 2003; Ramrattan et al., 1999; Wang, et al., 2008). The current study had most similar results with Wang et al. (2008), who had a prevalence of 19.9% of 8878 eyes. Number of subjects in the mentioned study was 4439 and was considered highest compared with other studies (Wang et al., 2008). Number of included subjects in the current study was 68 with inclusion of 64 eyes for right eyes and 63 eyes for left eyes (table 4-1). Demographics was most similar compared to Wang et al., (2008), except from the fact that their study population was Asian, and the current study was mostly Caucasians, although not recorded.

Jonas et al. (2003) reported lowest prevalence of beta parapapillary atrophy with 11.4% in an Asian population. The prevalence differed by 12.0% for right eye and 15.6% for left eye from the current study, and paradoxically, the number of subjects were close to the same for both studies, but the number of eyes used was not addressed in the study of Jonas et al. (2003). The latter could have explained the reason for different results between the studies if they only included 70 eyes in total, compared with the 127 eyes included in this study (table 4-1). Mean age was 47.5 years, along with refractive power range from -4.50D to +2.50D in the study of Jonas et al. (2003), compared with a higher mean age of 66.7 years and refractive power range from -11.00D to +8.25D in current study. These factors could explain why Jonas et al. (2003) had lower prevalence of beta parapapillary atrophy.

In two studies on Caucasians, Jonas et al. (1989) found a prevalence of 15.2% in 390 eyes and Ramrattan et al. (1999) found 13.0% in at least one eye out of 894 eyes. The prevalence of these studies was consistent with each other but differed slightly from the current study. Interesting aspects was that Ramrattan et al. (1999) had mean age similar to the current study but a higher mean refractive error (+1,27D), whilst Jonas et al. (1989) had a low mean age (44.4 years) and mean refractive powers similar to this study (table 4-2).

It is worth mentioning that the current study included self-reported glaucoma and did not register any cases that was diagnosed with glaucoma during examination. This could mean that the prevalence of glaucoma was even higher for this study, than the 4.4% reported, as glaucoma is associated with higher prevalence of beta parapapillary atrophy (Wang et al., 2008; Ramrattan et al., 1999). Glaucoma was not an exclusion criterion in this study, due to few cases. Another aspect worth mentioning is that methods used and the technology of retinal cameras available in the mentioned studies compared to this study are different. The retinal images in this study was digital, while the images from the first studies was analogue and used manual overlays (Jonas et al., 1989; Ramrattan et al., 1999), and so the quality and pixels available in the images may vary. As mentioned in next chapter, the definitions used for beta parapapillary atrophy might also be somewhat uncertain.

Overall, there were differences and similarities in prevalence and demographics between the mentioned studies and the current study, and there was no obvious reason for the differences between these studies and the current study. The highest prevalent study had the highest number of subjects and is considered to have the most reliable estimate (Wang et al., 2008). The current study had similar results.

Prevalence of beta parapapillary atrophy of both eyes was 21.7% in the current study. This was lower than for right and left eyes, but still higher than the available literature on prevalence in one eye. There are no studies to compare with for both eyes. The lower prevalence indicates that there are smaller chances for having beta parapapillary atrophy in both eyes than in one eye, and it would be interesting to see if it correlates with any ocular diseases that could manifest in one of the eyes, such as glaucoma, ocular hypertension or age-related macular degeneration.

### 5.1.1 Unclassified parapapillary atrophy and critical evaluation of current definition of beta parapapillary atrophy

In the current study, when beta parapapillary atrophy was not present, unclassified atrophy was present in 15.6% for right eyes and 15.9% for left eyes. In both eyes, 5.0% unclassified parapapillary atrophy was present when beta parapapillary atrophy was not present. Unclassified parapapillary atrophy was for this study defined as any parapapillary atrophy that could not be identified as normal retina, beta parapapillary atrophy or alpha parapapillary atrophy, nor as parts of the scleral ring, and the zone itself would appear atrophic. (table 3-2 and figure 3-6). Unclassified parapapillary atrophy has not been mentioned in the pertinent literature. It was simply registered in this study since it did not match any of the existing definitions on appearance of parapapillary atrophies in the literature (Dai et al., 2013; Guo et al., 2012; Jonas et al., 1989; Jonas et al., 2003; Lee et al., 2010; Lee et al., 2011; Park et al., 2010; Ramrattan et al., 1999; VanderBeek et al., 2010; Wang et al., 2008).

Although there is consistency in the definition on histological features of beta parapapillary atrophy (Curcio et al., 2000; Kubota et al., 1993), there seems to be an unprecise application of the definition on the appearance of beta parapapillary atrophy seen ophthalmoscopically in studies. The definition seems to be consistent with marked atrophy of RPE, or absence of RPE, and most studies mentions marked atrophy of choriocapillaris and thinning of chorioretinal tissues (Dai et al., 2013; Guo et al., 2012; Jonas et al., 1989; Jonas et al., 2003; Lee et al., 2010; Lee et al., 2011; Park et al., 2010; Ramrattan et al., 1999; VanderBeek et al., 2010; Wang et al., 2008). This is ophthalmoscopically seen as visible sclera (or a white area) with visible choroidal vessels (Dai, et al., 2013; Guo, et al., 2012; Jonas, et al., 1989; Jonas et al., 2003; Lee, et al., 2011; Park et al., 2010; Ramrattan, et al., 1999; Wang, et al., 2008). Some studies, although not regarding prevalence, left out parts of the definition, especially regarding visible choroidal blood vessels (Lee et al., 2010; VanderBeek et al., 2010), which is an important landmark in differentiations between ophthalmoscopically seen atrophies. Majority of the mentioned ophthalmoscopically studies, including this study, refers to well-established publications such as Jonas et al. (1989) or Ramrattan et at. (1999), or other studies based on their work, regarding definition of beta parapapillary atrophy. The paradox is that Jonas et al. (1989) also mentioned that beta atrophy could be seen as small grey fields on a whitish background, but this was never mentioned or specified as

inclusion or exclusion for any of the studies that referred to Jonas and associates (Jonas et al., 2003; Ramrattan et al., 1999; Wang et al., 2008). Also, none of the studies specified why they excluded the choroidal blood vessels as landmarks in their beta atrophy definition (VanderBeek et al., 2010; Lee et al., 2010). The small grey fields Jonas initially mentioned are most likely pigmentations in the choroid or sclera, as one could expect to see (Bergmanson, 2014), but the description of this appearance of the beta atrophy in operational definition has not been described by any studies.

In the current study, as an attempt to include the histological features (Curcio et al., 2000; Kubota et al., 1993) of beta parapapillary atrophy and variations of how it might look like operationally based on anatomy (Bergmanson et al., 2014), not only white sclera was included, due to the normal variation of appearance. The definition was a whitish or bright yellowish area, sometimes blending in with smaller or bigger darker patches within the same area, with transparency to one or several large visible choroidal vessels within parts or the whole beta zone (figure 3-6). The appearance of beta zones was compared with and distinguished from any other parapapillary zones or structures that could be mistaken for a beta parapapillary atrophy appearance (table 3-2).

According to images seen in the mentioned literature, there were no reason to believe that this study had included a too broad definition, as it simply just described the appearance of different variations of beta parapapillary atrophies, still being in line with the overall theoretical definition (Jonas et al., 1989; Ramrattan et al., 1999; Wang et al., 2008), that the majority of literature does not describe, but assumes. A more precise definition for ophthalmoscopically seen beta parapapillary atrophy is needed. It would be interesting to know if some of the differences in prevalence of beta is owed to the lack of standardized criteria for beta parapapillary atrophy.

### 5.1.2 Image quality of fundus photographs

Based on the grading scale for image quality of the fundus photographs in table 3-1, 3.0% of all images for right and left eye together had total quality grade 1 (poor quality), 66.7% had total quality grade 2 (intermediate quality) and 30.4% had total quality grade 3 (good quality). There was an insignificant difference between the eyes. Results for total image quality for right eyes and left eyes are listed in table 4-3. Since the quality scale was a 3-step scale, as assumed, the most images had intermediate quality, as there were only 3 criteria for discriminating between grades, and the

threshold for scoring a good-quality image was higher, and the threshold for scoring a poor-quality image was much lower, compared with an averaged-quality image. For right and left eyes regarding sharpness, 66.2% and 64.2% had grade 2, respectively, and 30.9% and 34.3% had grade 3, respectively. The fundus camera used in this study had a digital resolution of 4.5 microns +/- 7% (Kowa Company, 2010; Niko Corporation, 2008), but opacities in the camera medias and human eye medias results in that the human eye can only see certain fine details on a fundus image, optimally around 20 microns, correlating with a bundle of RNFL or large capillaries (Morisbakk, 2014; Tyler et al., 2003). Therefore, most images would get a grade 2 of sharpness. For exposure, the structures evaluated didn't seem to be influenced as much by the light as the sharpness. This was expected since the images was optimized with light levels before evaluating (Allen & Triantaphillidou, 2012). For right and left eyes regarding exposure, 19.1% and 19.4% had grade 2, respectively, and 80.9% and 79.1% had grade 3, respectively. It was not appropriate to compare the quality of images in this study with other studies, as the criteria differed (Bartling et al., 2009).

#### 5.1.2.1 Image quality and influence of results

Ramrattan et al. (1999) experienced that low-quality photographs caused the disc area to be measured larger. Other studies, including the current study, have excluded images due to poor image quality, and Ramrattan et al. (1999) described that interpolating of topographical results was done for images with poor quality (Ramratta et al., 1999). By excluding or interpolating data, the results will be influenced. In this study, prevalence for beta parapapillary in right and left eyes were done regarding image quality only with grade 2 and grade 3 to see if prevalence changed. Frequency of beta parapapillary atrophy with total image quality grade 2 was 24.4% for right eyes and 31.0% for left eyes. This means that prevalence for beta parapapillary atrophy was higher when only including grade 2, compared with prevalence of 23.4% for right eyes and 27.0% for left eyes grade 2 and 3 together. This could implicate some unwilling extrapolating or overestimating of results in the current study when image quality was not optimal.

Frequency of beta parapapillary atrophy with total image quality grade 3 was 21.1% for right eyes and 19.0% for left eyes. This means that prevalence for beta parapapillary atrophy was lower when only including grade 3, compared with prevalence of 23.4% for right eyes and 27% for left eyes with grade 2 and 3 together. This could indicate that high image quality makes the landmarks more defined when present, which makes it

easier to exclude border line cases of beta parapapillary atrophy. With total image quality grade 2, 45 eyes were included for right eye and 42 eyes were included for left eye. For total image quality grade 3, 19 eyes were included for right eye and 21 eyes were included for left eye. As seen, the selection of eyes was small, and there is too little data to be conclusive.

Image quality analyses of fundus photographs was not the main goal of this study, and significance testing of different grades was therefore not done, but consideration of quality of photographs was relevant for a certain evaluation of presence and distribution of parapapillary atrophy. Obtaining good quality images is important both in research and in clinical practice (Lamirel et al., 2012; Tyler et al., 2003). A similar, simple grading scale with belonging image templates, as shown in figure 3-3 for sharpness and figure 3-4 for exposure is recommended for clinicians to become more aware of image quality in their daily practice. See Annex 8 for a description of how to use the grading scale in general.

## **5.2 Distribution of frequencies of beta parapapillary atrophy around the optic nerve head by means of fundus photography**

Beta parapapillary atrophy occurred most often at 345 degrees with a prevalence of 25.0% for right eyes and at 330 degrees with a prevalence of 27.9% for left eyes. The lowest prevalence was at 75 degrees with a prevalence of 3.3%, thereafter a prevalence of 3.8% at 180-195 degrees in right eyes and from 150 to 225 degrees with prevalence of 0% in left eyes. Significance testing between eyes and sections was out of the scope of this study, especially since it was too little data, although it would have been interesting to compare.

Differences between left and right eye was small and distribution appeared relatively equal as seen in chart 4-1, with exception of the presence of parapapillary atrophy distributed around the whole optic nerve head for right eyes compared with a temporal crescent-form in left eyes, with less atrophy superior and inferior for left eyes compared with right eyes. The nasal side of left eyes had no presence of beta parapapillary atrophy, and the nasal side of right eyes had only 2 eyes with beta parapapillary atrophy



in an otherwise low number of eyes at the corresponding area, giving the slight difference between eyes on nasal side.

Overall, for right eyes, the distribution of frequencies was smallest in nasal region, with an even increase in prevalence towards superior region, with a small decrease at 75 degrees, before increasing further towards temporal region where it flattens out before peaking at 345 degrees and finally decrease evenly through inferior region to 225 degrees, where the curve goes rapid down to the flat, low area nasally again. For left eyes, the distribution of frequencies was flat with 0% from 225 degrees to 150 degrees on nasal side and increased slightly at 150 degrees, holding a flat curve through superior region to 60 degree, where it rapidly increased with a round curve through temporal region towards peak at 330 degrees, and then following the round, slight decreased curve to 285 degrees inferior, where it rapidly decreases towards nasal side.

The distribution around the optic nerve head for the mentioned studies regarding prevalence in one eye by means of fundus photo had similar prevalence for temporal side as for their overall prevalence in one eye (Jonas et al., 1989; Jonas et al. 2003; Wang et al., 2008). Jonas et al. (1989) found 14.7% in temporal section (2-4 o'clock in a left eye), 14.3% in inferior-temporal section (4-7 o'clock in a left eye), 13.4% in superior-temporal section (11-2 o'clock in a left eye) and 4.8% in nasal section (7-11 o'clock in a left eye). The same sections with belonging clock hours was used by the other studies. Jonas et al. (2003) found 11.4% in temporal, inferior-temporal and superior-temporal section, and 1.4% in nasal section. Wang et al. (2008) found a prevalence of 19.7% in temporal section, 16.3% in inferior-temporal section, 15.1% in superior-temporal section and 5.6% in nasal section. All studies had similar order of distribution of prevalence around the eyes, with highest prevalence in temporal section, followed by inferior, superior and nasal sections. This was similar for both eyes in the current study.

## **5.3 Distribution of frequencies of beta parapapillary atrophy around the optic nerve head by means of fundus photography and SD-OCT**

### **5.3.1 Frequency of beta parapapillary atrophy by means of SD-OCT**

For right eyes, the prevalence for beta parapapillary atrophy was 79.7%. For left eyes the prevalence was 65.1%. Prevalence for both eyes was 60.0%. Prevalence of beta parapapillary atrophy in current study, compared to other studies, was slightly above and just in between reported frequencies in one eye for right and left eyes, respectively. (Hayashi et al., 2012; Lee et al., 2010; Zhang et al., 2018).

Prevalence of beta parapapillary atrophy in the current study for SD-OCT differed from the ophthalmoscopically results presented. This relation between image modalities is similar when comparing ophthalmoscopically studies with OCT-studies in literature (Hayashi et al., 2012; Jonas et al., 1989; Jonas et al., 2003; Lee et al., 2010; Wang et al., 2008; Zhang et al., 2018). For right eyes, the prevalence of parapapillary atrophy observed on fundus photography and SD-OCT was 23.4% and 79.7% respectively. For left eyes, this relation was 27.0% and 65.1%, respectively. Even though there were some difference in prevalence between right and left eyes in fundus photo, they were insignificant. In SD-OCT, the difference in prevalence was even higher between eyes. Fundus photo had highest prevalence of beta parapapillary atrophy in left eye, whilst SD-OCT had highest prevalence in right eye.

### **5.3.2 Distribution of frequencies of beta parapapillary atrophy around the optic nerve head by means of SD-OCT**

Beta parapapillary atrophy was most frequent at 345 degrees with a prevalence of 72.4 for right eyes and at 15 degrees for left eye with a prevalence of 67.3%. The lowest prevalence was 20% at 195 degrees for right eyes and 21.4% at 225 degrees for left eyes. Zhang et al. (2018), found that beta parapapillary atrophy present in eyes, occurred most prevalent in temporal region and least prevalent (0%) in nasal region, in eyes with beta. It is worth mentioning that he only measured one point, maybe explaining why he had 0%.

In general, for right eyes, the distribution of prevalence was lowest nasally, and increased with a peak at 135 towards superior region, before increasing further towards highest peak at 345 in temporal region, thereafter decreasing gently towards inferior region, with a notch at 285, before decreasing towards nasal side. For left eyes, the prevalence was lowest at 225 degrees in the inferior-nasal region, with an even curved increase towards a peak at 90 degrees superior, with a small decrease at 60 degrees before increasing to the highest peak at 15 degrees, and then slightly decrease towards inferior region, with a small peak before decreasing towards nasal side.

A similar distribution was seen on fundus photography, as described in chapter 5.2. Even though the prevalence was lower for the distribution of beta parapapillary atrophy on fundus images, the distribution was corresponding with the distribution of the higher frequencies around the optic nerve head for SD-OCT. The distribution of prevalence of beta parapapillary atrophy was highest for the temporal region on both image modalities in both eyes and lowest for the nasal region in both eyes on both image modalities. Findings are similar with the literature (Jonas et al., 1989; Jonas et al., 1999; Wang et al., 2008; Zhang et al., 2018). However, there were some exceptions, such as the missing presence of beta seen on fundus photo nasal in left eyes, where the SD-OCT revealed that there was beta present. Also, a notch seen on SD-OCT in right eye, was not present on distribution on fundus photo at 285 degrees in right eyes.

## **5.4 Distribution of frequencies of distal border of beta parapapillary atrophy by means of fundus photography and SD-OCT**

For eyes with beta parapapillary atrophy, the distribution of frequencies of overlapping distal borders of parapapillary atrophy was highest in the superior-temporal region in right and left eyes. The highest prevalence of overlapping distal borders in right eyes was 28.6% at 60 and 345 degrees. For left eyes, the highest prevalence of overlapping distal borders was 54.5% at 30 degrees. For right eyes, the prevalence of overlapping distal border was also observed in superior-nasal area, although the percentage might be higher due to the low selection of eyes.

The distribution of frequencies of OCT-defined distal border of parapapillary atrophy placed on the inside of the fundus photo-defined distal border was highest in the

inferior-temporal region in both eyes. For right eyes, there was some distribution of frequencies in nasal region as well. The highest prevalence of OCT-defined distal border of beta parapapillary atrophy placed on the inside was 77.8% at 300 and 315 degrees for right eyes. For left eyes, the highest prevalence was 72.7% at 315 degrees. Overall, OCT-defined distal border placed on the inside of the fundus-defined distal border had highest frequencies compared with overlapping distal borders and the OCT-defined distal border placed outside of the fundus-defined distal border.

The distribution of frequencies of beta parapapillary atrophy with an OCT-defined distal border located on the outside of the fundus photo-defined distal border of the beta parapapillary atrophy was highest in the superior-temporal region for right and left eyes. The highest prevalence of OCT-defined distal border of beta parapapillary atrophy placed on the outside of the fundus photo-defined distal border was 33.3% for right eyes and 30.8% for left eyes at 15 degrees. Overall, OCT-defined distal border placed on the outside of the fundus-defined distal border occurs in fewer sections around the optic nerve head than overlapping distal borders and the OCT-defined distal border placed inside of the fundus-defined distal border.

Park et al. (2010) found that the distal border of parapapillary atrophy seen on FD-OCT and fundus photographs overlapped in 65.0% of images with beta present. Further, they found that the OCT-defined distal border placed on the inside of fundus photo-defined distal border was present in 35% of images with beta present (Park et al., 2010). Their study did only investigate temporal region and included eyes only with beta parapapillary atrophy (and glaucoma). Note that the percentage is not comparable with this study, but their findings suggests that the distal border is relatively easy to overlap by the mean of both image modalities (Park et al., 2010). The tendency was different in this study, as the OCT-defined distal border was mostly placed on the inside of the fundus photo-defined distal border. Park et al. (2010) explained this tendency with the presence of visible RPE on OCT, not having enough pigment to be seen on fundus photographs (Park et al., 2010). Clinically, this means that the detection of the distal border of beta atrophy seen on fundus images can be placed more peripherally than on OCT. Although the distal border of beta parapapillary atrophy has been proven to be easy to define (Tuulonen et al., 1996), ophthalmoscopically observed distal border might not be truly correct. In clinical practice, fundus photo should be complimented with OCT in defining parapapillary atrophy, although, borders might be unverified is

some cases. The current study had a great amount of unverified distal borders of beta parapapillary atrophy in both eyes (chart 4-2 and 4-3), that was due to misalignment of IR-images or other unverified reasons as described.

Distribution in mainly temporal and inferior-temporal region for the different outcomes of distal border of parapapillary atrophy is seen in context with the tendency for similar distribution of frequencies in the regions for presence of parapapillary atrophy.

## **5.5 Study limitations**

A main limitation for the study was the low number of subjects and eyes. only 68 subjects were included. This resulted in high confidence intervals, in which can give a more unsecure estimate of the actual value in the target population, compared to larger studies with more subjects. For sections in radial scan on IR-image and when overlapped on fundus photo, even less sections were included due to misaligning of IR-images and shadowing or blocking of relevant area due to blood vessels on both IR- and fundus images, especially in inferior and superior sections. Exclusion of IR-images could possibly have been reduced if more frequently quality assurance had been done during examination. This is important when collaborating in team with other observers. For fundus photographs, it was not as many exclusions regarding quality as there were exclusion due to misalignment on IR-images. Significance testing was not done for the comparing between frequencies and demographical data, nor between the sections on frequencies for beta parapapillary trophy. This was due to few subjects.

A second limitation was that during data collection and analyses, mostly, the right eye was examined before left eye in a systematical approach, which could have caused a learning effect that would influence results between eyes. Also, the study was not entirely masked for the main observer. Although the intention was to blind the main observer from the image analyses regarding OCT to avoid confirmation bias, the main observer had been collecting the same data for some of the subjects.



## 6 Conclusion

Prevalence of beta parapapillary atrophy by means of fundus photography was 23.4% for right eyes, 27.0% for left eyes and 21.7% for both eyes. The latter is a relevant finding for clinical practice, since it indicates that the atrophy is not always present in both eyes. By means of fundus photography, for both right and left eyes, atrophies were most prevalent in temporal region, followed by inferior region before superior region and finally nasal region. This concurs with pertinent literature.

Distribution of frequencies of beta parapapillary atrophy by means of fundus photography and SD-OCT corresponded with each other around the optic nerve head, although overall prevalence was lower for fundus photo and higher for SD-OCT. Atrophies were most prevalent for the temporal region and least prevalent for nasal region in both eyes. This concurs with pertinent literature. Unique for this study was that both image modalities showed a similar distribution of frequencies in the same study population.

Overlapping distal borders of parapapillary atrophy defined by SD-OCT and fundus photography was most frequent in superior-temporal region for both eyes. OCT-defined distal border placed on the inside of fundus photo-defined distal border was most frequent in inferior-temporal region in both eyes. OCT-defined distal border placed on the outside of fundus photo-defined distal border was most frequent in superior-temporal region in both eyes. In general, there was much higher frequencies of the OCT-defined distal border on the inside of fundus photo-defined distal border, than the two other outcomes. This differs from the pertinent literature. Unique for this study was that frequencies of distal border of beta parapapillary atrophy in both image modalities was investigated around the whole optic nerve head in both eyes.





## References

- Abràmoff, M. D., Garvin, M. K., & Sonka, M. (2010). Retinal Imaging and Image Analysis. *IEEE Reviews in Biomedical Engineering*, 3, 169-208.  
doi: 10.1109/RBME.2010.2084567
- Allen, E. & Triantaphillidou, S. (2012). *The Manual of Photography and Digital Imaging* (10<sup>th</sup> Edition). Focal Press. ISBN: 9780240520377
- Anon, E. & Anon, J. (2010). *Photoshop CS5 for nature photographers : a workshop in a book* (1<sup>st</sup> edition). Indianapolis, Ind.: Wiley. ISBN: 1-282-68889-8
- Bartling, H., Wanger, P., & Martin, L. (2009). Automated quality evaluation of digital fundus photographs. *Acta Ophthalmologica*, 87(6), 643-647.
- Bergmanson, J.P.G. (2014). *Clinical Ocular Anatomy and Physiology*, 21<sup>st</sup> edition, Texas, USA.
- Carl Zeiss Meditec. (2014). *Cirrus HD-OCT, Models 500 and 5000 – Documentation set*. Dublin, CA. [User manual].
- Curcio, C.A., Saunders, P.L., Younger, P.W. & Malek, G. (2000). Peripapillary Chorioretinal Atrophy – Bruch`s membrane Changes and Photoreceptor Loss. *Ophthalmology*, 107 (7), 334-343. doi: 10.1016/S0161-6420(99)00037-8
- Dai, Y., Jonas, J.B., Huang, H., Wang, M. & Sun, X. (2013). Microstructure of Parapapillary Atrophy: Beta Zone and Gamma Zone. *Investigative Ophthalmology and Visual Science*, 54(3), 2013-2018. doi: 10.1167/ivos.12-11255
- Felleskatalogen. (no year). Tropikamid Minims – Bausch & Lomb U.K. Ltd. Available from: <https://www.felleskatalogen.no/medisin/tropikamid-minims-bausch-&-lomb-u-k-ltd-564867> [Downloaded 05.04.2019].
- Guo, Y., Wang Y.X., Xu, L. & Jonas, J.B. (2012). Five-Year Follow-Up of Parapapillary Atrophy: The Beijing Eye Study. *PLoS ONE*, 7(5), e32005.  
doi: 10.1371/journal.pone.0032005
- Hayashi, K., Tomidokoro, A., Lee, K.Y.C, Konno, S., Saito, H., Mayama, C., Aihara, M., Iwase, A. & Araie, M. (2012). Spectral-Domain Optical Coherence Tomography of  $\beta$ -zone Peripapillary Atrophy: Influence of Myopia and Glaucoma. *Investigative Ophthalmology and Visual Science*, 53(3), 1499-1505.  
doi: 10.1167/ivos.11-8572
- Helsepersonelloven. (1999). Lov om helsepersonell m.v. (LOV-1999-07-02-64). Available from: <https://lovdata.no/dokument/NL/lov/1999-07-02-64> [Downloaded

05.04.2019].

- Huang, D., Swanson, E.A., Lin, C.P., Schuman, J.S., Stinson, W.G., Chang, W., ...Fujimoto, J.G. (1991). Optical Coherence Tomography. *Science*, 254(5035), 1178-1181. ISSN: 00368075
- Jonas, J.B., Jonas, S.B., Jonas, R.A., Holbach, L., Dai, Y., Sun, X. & Panda-Jones, S. (2012). Parapapillary Atrophy: Histological Gamma Zone and Delta Zone. *PLoS ONE*, 7 (10), e47237. doi: 10.1371/journal.pone.0047237
- Jonas, J.B., Nguyen, X.N., Gusek, G.C. & Naumann, G.O.H. (1989). Parapapillary Chorioretinal Atrophy in Normal and Glaucoma Eyes. *Investigative Ophthalmology & Visual Science*, 30(5), 908-918. ISSN: 01460404
- Jonas, J.B., Thomas, R., George, R., & Berenshtein, J.M. (2003). Optic disc morphology in south India: the Vellore Eye Study. *British Journal of Ophthalmology*, 87(2), 189-196. doi: 10.1136/bjo.87.2.189
- Kim, M., Kim, T., Weinreb, R.N. & Lee, E.J. (2013). Differentiation of Parapapillary Atrophy Using Spectral-Domain Optical Coherence Tomography. *Ophthalmology*, 120(9), 1790-1797. doi: 10.1016/j.ophtha.2013.02.011
- Kowa Company. (2010). *2D/3D Non-mydratic Retinal Camera: Kowa nonmyd WX 3D: Instruction manual*. [User manual]. Japan. Available from: <https://ophthalmic.kowa-usa.com/wp-content/themes/kowa-eyecare/pdf/Kowa-Ophthalmic-Diagnostics-Nonmyd-WX-3D-Manual.pdf> [Downloaded 05.04.2019].
- Kubota, T., Jonas, J.B. & Naumann, G.O.H. (1993). Direct clinico-histological correlation of parapapillary chorioretinal atrophy. *British Journal of Ophthalmology*, 77(2), 103-106. doi: http://dx.doi.org/10.1136/bjo.77.2.103
- Lamirel, C., Bruce, B.B, Wright, D.W., Delaney, K.P., Newman, N.J. & Biousse, V. (2012). Quality of Nonmydratic Digital Fundus Photography Obtained by Nurse Practitioners in the Emergency Department: The FOTO-ED Study. *American Academy of Ophthalmology*, 119(3), 617-624. doi: 10.1016/j.ophtha.2011.09.013
- Lee, K.Y.C., Tomidokoro, A., Sakata, R., Konno, S., Mayama, C., Saito, H., Hayasbi, K., Iwase, A. & Araie, M. (2010) Cross-sectional anatomic Configurations of Peripapillary Atrophy Evaluated with Spectral Domain-Optical Coherence Tomography. *Investigative Ophthalmology & Visual Science*, 51(2), 666-671. doi: 10.1167/ivos.09-3663
- Lee, E.J., Kim, T-W., Weinreb, R.N., Park, K.H., Kim, S.H. & Kim, D.M. (2011).  $\beta$ -Zone parapapillary atrophy and the rate of retinal nerve fiber layer thinning in

- glaucoma. *Investigative Ophthalmology & Visual Science*, 52(7), 4422-4427.  
doi: 10.1167/iovs.10-6818.
- Morisebakk, T.L. (2014). *Measurements of the relationship between retinal structure and visual function in normal healthy subjects*. (PhD thesis). Norwegian University of Life Sciences: Department of Mathematical Sciences and Technology, Ås.
- Miki, A., Ikuno, Y., Weinreb, R.N., Asai, T., Usui, S. & Nishida, K. (2019). En Face Optical Coherence Tomography Imaging of Beta and Gamma Parapapillary Atrophy in High Myopia. *American Academy of Ophthalmology*, 2(1), 55-62.  
doi: <http://dx.doi.org/10.1016/j.ogla.2018.11.008>
- Miki, A., Ikuno, Y., Weinreb, R.N., Yokoyama, J., Asai, T., Usui, S. & Nishida, K. (2017). Measurements of the parapapillary atrophy zones in en face optical coherence tomography images. *PLoS ONE*, 12(4), e0175347.  
doi: 10.1371/journal.pone.0175347
- Nikon Corporation. (August 2008). Imaging Products: Specifications: D90. Available from: <https://imaging.nikon.com/lineup/dslr/d90/spec.htm> [Downloaded 05.04.2019].
- Norwegian electrotechnical publication (2014) Safety of laser products – Part 1: Equipment classification and requirements (NEK IEC 60825-1:2014)
- Olsen, D. Ø. (2018). Etterlyst: Flere spesialister. *Optikeren*, 2018(5), page 26-28.  
Available from: <https://www.optikerne.no/pages/optikeren/issues/optikeren201805.pdf> [Downloaded 26.04.2019].
- Park, S.C., De Moares, C.G.V., Tello, C., Liebmann, J.M. & Ritch, R. (2010). In-Vivo Microstructural Anatomy of  $\beta$ -Zone Parapapillary Atrophy in Glaucoma. *Investigative Ophthalmology and Visual Science*, 51(12), 6408-6413.  
doi: 10.1167/iovs.09-5100
- Pasient- og brukerrettighetsloven. (1999). Lov om pasient- og brukerrettigheter (LOV-1999-07-02-63). Available from: <https://lovdata.no/dokument/NL/lov/1999-07-02-63> [Downloaded 05.04.2019].
- Ramrattan, R.S., Wolfs, R.C.W., Jonas J.B., Hofman, A. & de Jong, P.T.V.M. (1999). Determinants of Optic Disc Characteristics in a General Population: The Rotterdam Study. *Ophthalmology*, 106(8), 1588-1596. doi: 10.1016/SO161-6420(99)90457-8
- Starengi, G., Sada, S., Chakravarthy, U. & Spaide, R.F. (2014). Proposed Lexicon for Anatomic Landmarks in Normal Posterior Segment Spectral-Domain Optical Coherence Tomography: The IN•OCT Consensus. *Ophthalmology*, 121(8), 1572-

1578. doi: 10.1016/j.ophttha.2014.02.023

Tuulonen, A., Jonas, J.B., Välimäki, S., Alanko, H.I. & Airaksinen, J. (1996).

Interobserver Variation in the Measurements of Peripapillary Atrophy in Glaucoma. *Ophthalmology*, 103(3), 535-541. doi: 10.1016/S0161-6420(96)30661-1

Tyler, M.E., Saine, P.J. & Bennet, T.J. (2003). *Practical Retinal Photography and Digital Imaging Techniques*. Butterworth-Heinemann, Philadelphia, Pennsylvania, USA.

Universitetet i Sørøst-Norge. (no year). Nasjonalt senter for optikk, syn og øyehelse.

Forskningsprosjekt for diabetes, syn og øyehelse. Available from:

<https://www.usn.no/forskning/hva-forsker-vi-pa/synsvitenskap/nasjonalt-senter-for-optikk-syn-og-oyehelse/forskningsprosjekter/diabetes-syn-og-oyehelse/>

[Downloaded 26.04.2019].

VanderBeek, B.L., Smith, S.D & Radcliffe, N.M. (2010). Comparing the detection and agreement of parapapillary atrophy progression using digital optic disk photographs and alternation flicker. *Graefe's Archive for Clinical and Experimental Ophthalmology*, 248(9), 1313-1317. doi: 10.1007/s00417-010-1376-z

Vianna, J.R., Malik, R., Danthurebandara, V.M., Sharpe, G.P., Belliveau, A.C., Shuba, L.M., Chauhan, B.C. & Nicoleta, M.T. (2016). Beta and Gamma Peripapillary Atrophy in Myopic Eyes With and Without Glaucoma. *Investigative Ophthalmology and Visual Science*, 57(7), 3103-3111. doi: 10.1167/iovs.16-19646

Wang, Y., Xu, L., Yang, H., Ma, Y. & Jonas, J.B. (2008). Peripapillary atrophy in elderly Chinese in rural and urban Beijing. *Eye*, 22(2), 261-266. doi: 10.1038/sj.eye.6702601

Zhang, Q., Wang, Y.X., Wei, W.B., Xu, L. & Jonas, J.B. (2018). Parapapillary Beta Zone and Gamma Zone in a Healthy Population: The Beijing Eye Study 2011. *Investigative Ophthalmology and Visual Science*, 59(8), 3320-3329. doi: 10.1167/iovs.18-24141

## List of figures, tables and charts

<i>Figure 1-1 Retinal image of optic nerve head with adjacent visible sclera surrounded by evenly coloured retina.</i> .....	12
<i>Figure 3-1 Data storage</i> .....	22
<i>Figure 3-2 Illustration of infrared image</i> .....	25
<i>Figure 3-3 Combinations of names for images saved in different stages throughout the analyses</i> .....	26
<i>Figure 3-4 Example images for thresholds for sharpness grade 1-3 in fundus photographs, when exposure is optimal</i> .....	28
<i>Figure 3-5 Example images for thresholds for exposure grade 1-3 in fundus photographs, when sharpness is optimal</i> .....	29
<i>Figure 3-6 Appearance of beta parapapillary atrophy</i> .....	31
<i>Figure 3-7 Marking of distal border of parapapillary atrophy</i> .....	33
<i>Figure 3-8 Markings of OCT-defined border on a transparent IR-image overlaid an underlying fundus image</i> .....	36
<i>Table 3-1 Grading scale of total image quality</i> .....	27
<i>Table 3-2 Differentiation of retinal zones.</i> .....	32
<i>Table 3-3 Categories for registration of Distal border of beta parapapillary atrophy.</i>	37
<i>Table 4-1 Exclusion and inclusion in the statistical analyses</i> .....	41
<i>Table 4-2 Demographical results of gender, age and refractive error</i> .....	42
<i>Table 4-3 Frequencies of different gradings of sharpness, exposure and total image quality for right and left eye</i> .....	42
<i>Table 4-4 Distribution of frequencies of beta and unclassified parapapillary atrophy around the optic nerve head in right and left eye based on fundus photo</i> .....	45
<i>Table 4-5 Distribution of frequencies of beta parapapillary atrophy around the optic nerve head in right and left eye based on SD-OCT</i> .....	46
<i>Table 4-6 Distribution of frequencies of distal border of beta parapapillary atrophy in right and left eyes</i> .....	48
<i>Chart 4-1 Distribution of frequencies of beta parapapillary atrophy surrounding the optic nerve head on fundus photo and SD-OCT in right and left eye:</i> .....	44
<i>Chart 4-2 Distribution of frequencies of distal border of beta parapapillary in right eye</i> .....	47

*Chart 4-3 Distribution of frequencies of distal border of beta parapapillary in left eye.*

..... 47

## **Annexes**

**Annex 1:** *Participation in DVOH project and consent form*

**Annex 2:** *Protocol: Fundus Photography*

**Annex 3:** *Protocol: OCT*

**Annex 4:** *Protocol: Export and storage of raw images*

**Annex 5:** *Registration form*

**Annex 6:** *Protocol: ImageJ*

**Annex 7:** *Table: Distribution of frequencies of “No beta atrophy”, “Beta with certain border”, “Beta with uncertain border” and “Unclassified atrophy” in right and left eye.*

**Annex 8:** *How to use grading scale for total image quality of fundus images*

# Annex 1:

## Diabetes, syn og øyehelse

### FORESPØRSEL OM DELTAKELSE I FORSKNINGSPROSJEKTET

## Diabetes, syn og øyehelse

Dette er et spørsmål til deg om å delta i ett forskningsprosjekt hvor formålet med prosjektet er undersøke hvordan synsfunksjon, øyehelse og livskvalitet påvirkes hos personer som har type 2 diabetes, og vurdere hvilke undersøkelsesmetoder som er mest effektive for å avdekke syn- og øyeproblemer hos optikere. Resultatene fra prosjektet forventes å gi et vesentlig bidrag til å gjøre optikere i bedre stand til å avdekke syn- og øyeproblemer og håndtere disse målrettet og effektivt, og redusere antallet henvisninger til øyelege.

Du forespørres om å delta fordi du har diabetes type 2 og har blitt invitert gjennom Nasjonalt senter for optikk, syn og øyehelse (NOSØ), Diabetesforbundets lokallag i Buskerud, Telemark og Vestfold, eller gjennom optikere i disse fylkene. Forskningsprosjektet og alle undersøkelser gjennomføres ved NOSØ, Institutt for optometri, radiografi og lysdesign, Fakultet for helse og sosialvitenskap, Høgskolen i Sørøst-Norge, avdeling Kongsberg.

### HVA INNEBÆRER PROSJEKTET?

Ved deltakelse i prosjektet vil du bli bedt om å fylle ut spørreskjemaer som avdekker syn- og øyesymptomer og din oppfattelse av livskvalitet knyttet opp mot syn. Du vil gjennomgå undersøkelser som er etter Norges Optikerforbund's retningslinjer. Dette innebærer blant annet: innledende samtale og spørsmål, måling av synsevne, utmåling av eventuelle synsfeil på avstand, samt mikroskopiundersøkelse av fremre og bakre del av øynene. Det vil bli målt øyetrykk, samt at netthinnen din blir avbildet med forskjellige instrumenter. Noen målinger krever at vi drypper med pupilleutvidende dråper. Undersøkelsene som inngår i prosjektet er fordelt over tre besøk, og tidsforbruket vil være ca. 2 timer for hvert besøk. Vi vil også be deg om å komme tilbake til oppfølgende undersøkelse etter 1, 5 og 10 år.

I prosjektet vil vi innhente og registrere opplysninger om deg. Dette er opplysninger som kjønn, alder og resultater fra spørreskjemaer og kliniske tester. Dine opplysninger og resultater vil under prosjektperioden være knyttet til en navneliste gjennom en kode. Kodenøkkel slettes når datainnsamlingen er avsluttet. Opplysningene som lagres vil i etterkant ikke kunne knyttes til din person.

### MULIGE FORDELER OG ULEMPER

Som deltaker i prosjektet får du gjennomført en grundig syn- og øyeundersøkelse. Undersøkelsen inkluderer undersøkelse av tårefilmen, det ytre øyet og netthinnen, og undersøkelser av hvor godt du ser. Det vil bli gitt veiledning og råd som kan gi deg best mulig syn og lindre eventuelle plager for eksempel hvis du har tørre øyne. Dersom det oppdages noen unormale funn, vil vi følge opp dette og sørge for at du får informasjon og eventuell henvisning til øyelege eller lege.

Det er ikke knyttet risiko, betydelig ubehag eller bivirkninger til noen av undersøkelsene. Det vil være nødvendig å bruke øyedråper (Tropikamid 0,5% minims) for å utvide pupillene. Dette kan av noen oppleves litt



## Diabetes, syn og øyehelse

ubehagelig da dråpene kan svi noe, og at man blir mer lysømfintlig i etterkant. Effekten av øyedråpene vil avta gradvis og opphører helt etter noen timer. Du bør ikke kjøre bil før synet er normalisert.

Det er gratis å delta i prosjektet.

### FRIVILLIG DELTAKELSE OG MULIGHET FOR Å TREKKE SITT SAMTYKKE

Det er frivillig å delta i prosjektet. Dersom du ønsker å delta, undertegner du samtykkeerklæringen på siste side. Du kan når som helst og uten å oppgi noen grunn trekke ditt samtykke. Dette vil ikke få konsekvenser for din videre behandling ved NOSØ. Dersom du trekker deg fra prosjektet, kan du kreve å få slettet innsamlede prøver og opplysninger, med mindre opplysningene allerede er inngått i analyser eller brukt i vitenskapelige publikasjoner. Dersom du senere ønsker å trekke deg eller har spørsmål til prosjektet, kan du kontakte førsteamanuensis Tove Lise Morisbakk (tlf 31 00 97 55, [tovelm@usn.no](mailto:tovelm@usn.no)) eller førsteamanuensis Vibeke Sundling (tlf 31 00 89 55, [vibeke.sundling@usn.no](mailto:vibeke.sundling@usn.no)).

### HVA SKJER MED INFORMASJONEN OM DEG?

Informasjonen som registreres om deg skal kun brukes slik som beskrevet i hensikten med studien. Du har rett til innsyn i hvilke opplysninger som er registrert om deg og rett til å få korrigert eventuelle feil i de opplysningene som er registrert.

Alle opplysningene vil bli behandlet uten navn og fødselsnummer eller andre direkte gjenkjenningse opplysninger. En kode knytter deg til dine opplysninger gjennom en navneliste.

Prosjektleder, førsteamanuensis Vibeke Sundling, Institutt for optometri, radiografi og lysdesign, Fakultet for helse og sosialvitenskap, Høgskolen i Sørøst-Norge ved Nasjonalt Senter for optikk syn og øyehelse har ansvar for den daglige driften av forskningsprosjektet og at opplysninger om deg blir behandlet på en sikker måte. Informasjon om deg vil bli anonymisert eller slettet senest fem år etter prosjektslutt. Prosjektleder kan kontaktes på tlf: 924 24 360 eller [vibeke.sundling@usn.no](mailto:vibeke.sundling@usn.no).

### FORSIKRING

Pasientskadeloven.

### GODKJENNING

Prosjektet er godkjent av Regional komite for medisinsk og helsefaglig forskningsetikk, (2018/804).

SAMTYKKE TIL DELTAKELSE I PROSJEKTET

JEG ER VILLIG TIL Å DELTA I PROSJEKTET

---

Sted og dato

Deltakers signatur

---

Deltakers navn med trykte bokstaver

Jeg bekrefter å ha gitt informasjon om prosjektet

---

Sted og dato

Signatur

## Annex 2:

### Protocol: Fundus photography

Instrument: *Kowa nonmyd Wx 3D*

Location: *Goldmann lab (2.floor)*

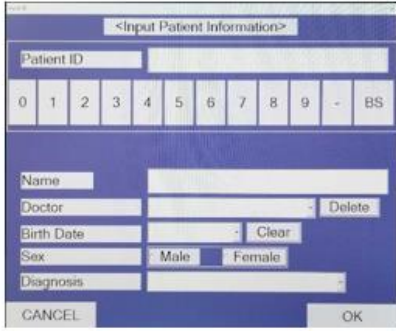
#### Preparations

##### Switch on PC and start Acquisition program

- Username: .\2311
- Password: *Krona2017*
- Click on icon VK2

##### Registration of subjects

- Click "Capture" in the fan in the data program, followed by "Input Data..."
- Register the patient ID, name, date of birth and gender in the boxes, as seen in the picture.
- Press "OK" and continue with the rest of the protocol.



##### Switch on TV and display acquisition program on screen

- Use remote control for TV to switch it on
- Click on the frame of the acquisition program and hold down; Move the image to the left until it appears on the TV screen.
- Screens may be reset by pressing Ctrl + N.

##### Switch on Camera and prepare for use

- Untighten the moving component fixing screw.
- Remove lens cap and check clearness of the lens.  
Use dust bellow and/or lens brush to remove particles.  
If necessary, use dedicated lens paper and solution to remove stain by gentle rotational movement along a spiral path from centre to periphery of the lens.

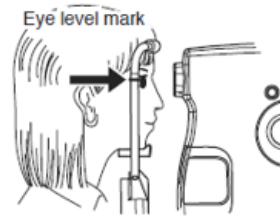
##### Choose sequence of eyes

- Right followed by left or Left followed by right selected from log
- Register and cross out in log
- Acquisition will be in the same sequence for both eyes:  
**(1) Normal Disc, (2) Normal Macula and (3) Stereo Disc**

##### Preparation for photography

- Clean chin- and headrest with alcohol
- Describe procedure

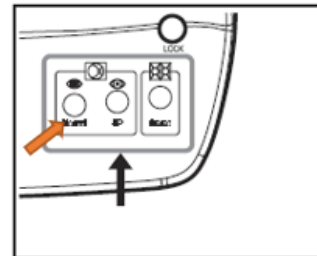
- Reduce illumination in room (turn off all the main light by pressing the light knob "0" and leave the small light at the computer desk on.)
- Occlude subjects eye with eye patch if necessary (e.g. tropia etc.)
- Position subject and align head
- Give instructions before each picture is taken:
  - Tell the patient to blink normal until you give further instructions.
  - When aligning the camera in anterior part of eye, tell the patient to look at the internal fixation target (green dot), and make patient aware that the target moves as you switch to alignment of posterior part.
  - Before taking the final picture, tell the patient to blink once or twice and then keep their eyes open.
- Quality check every photo as described in sections "QUALITY CHECK".



## Acquisition: (1) Normal Disc

### SELECTING PHOTOGRAPHY MODE = NORMAL

Select a photography mode by pressing "Normal", "SP", or "Stereo" button.



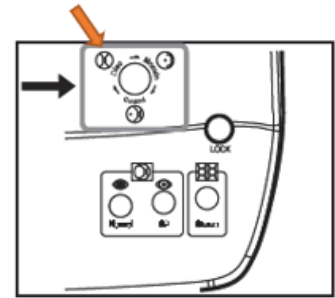
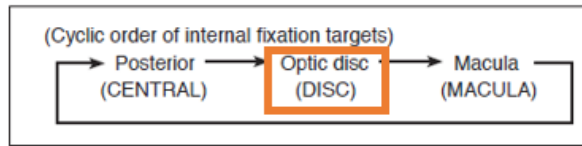
Check that the mode you have selected is shown on the upper left corner of LCD monitor.

Normal mode	SP mode	Stereo mode
<p>NORMAL ANTERIOR 45°</p> <p>EXP: 0 CENTRAL</p>	<p>SMALL PUPIL ANTERIOR 45°</p> <p>EXP: 0 CENTRAL</p>	<p>STEREO ANTERIOR 20° x 27°</p> <p>EXP: 0 DISC</p>

## SELECTING FIXATION TARGET = DISC

Use internal fixation target selection button to select an internal fixation target that you use for retinal observation.

Continuously pressing the button cycles through the targets as shown in the figure below.



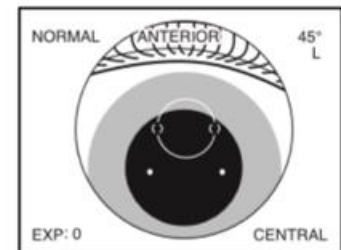
## ALIGNMENT IN ANTERIOR SEGMENT OBSERVATION

Instruct the patient to look straight ahead.

Perform the step described in "6.1.5 Alignment". Ask the patient to look straight ahead at the green illuminating spot when the patient's pupil becomes shown in the center of LCD monitor.

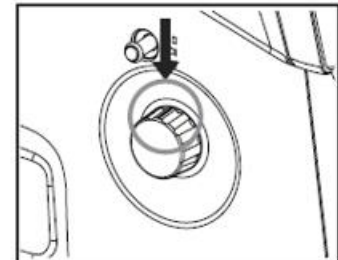
### 6.1.5 Aligning

Pull the optical component as close as possible to you and move the optical head base leftward/rightward or upward/downward in order to capture the pupil at the center of the LCD monitor.



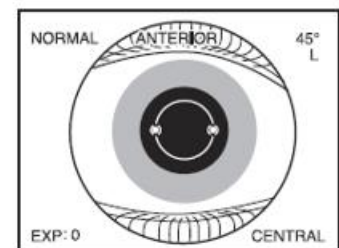
Beginning of alignment

Rotate focusing knob until the black line engraved on the knob faces upwards.



Focusing knob position

After the pupil image is captured successfully, move the optical head base forward until two working dots come in two pairs of round brackets "( )".



Alignment completed

## CHECK PUPIL DIAMETER AND RISK OF EYELID INTRUSION

Check the condition of dilation by comparing the patient's pupil diameter against the pupil diameter aid.

Change the photography light intensity as required depending on the mydriatic state.

If the patient's pupil diameter is smaller than that shown by the pupil diameter aid, press SP mode button to proceed to small pupil photography.

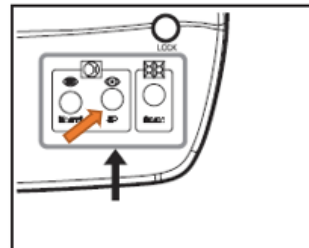
Photography light intensity	0	+1	Insufficient for photography
Normal mode Stereo mode Pupil diameter: φ 4 mm or greater			
SP mode Pupil diameter: φ 3.5 mm to 4 mm			

Register whether the pupil size fulfils requirement for NORMAL mode with optimal pharmacological mydriasis (max given dose).

If requirements for NORMAL mode is not obtained, select SP (Small Pupil) mode. In SP mode the acquisition sequence will be restricted to (1) Normal Disc and (2) Normal macula.

### SELECTING PHOTOGRAPHY MODE = SP

Select a photography mode by pressing "Normal", "SP", or "Stereo" button.



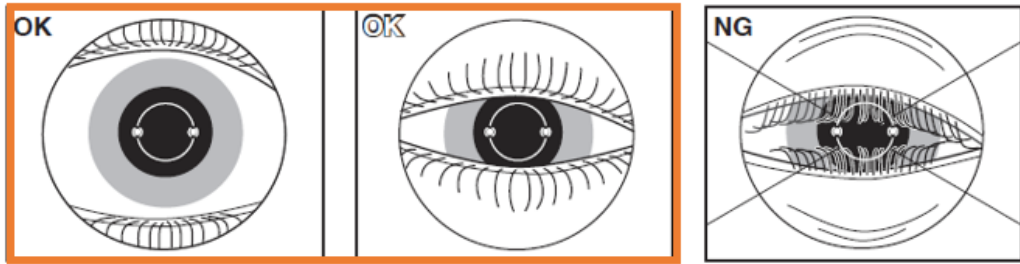
Check that the mode you have selected is shown on the upper left corner of LCD monitor.

Normal mode	SP mode	Stereo mode
<p>NORMAL ANTERIOR 45°</p> <p>EXP: 0 CENTRAL</p>	<p>SMALL PUPIL ANTERIOR 45°</p> <p>EXP: 0 CENTRAL</p>	<p>STEREO ANTERIOR 20° x 27°</p> <p>EXP: 0 DISC</p>

The eyelids or eyelashes intruding the pupil area interferes photography.

In such a case,

- Instruct the patient to widely open his or her eyes, or
- You or your assistant help the patient keep the eye wide open.

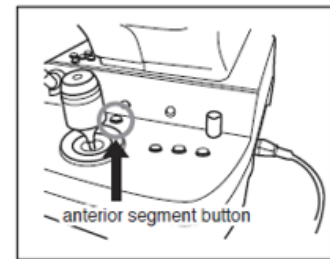


Register whether or not the eyelids fulfills requirement for NORMAL mode or SP mode if selected, and if this requires your help.

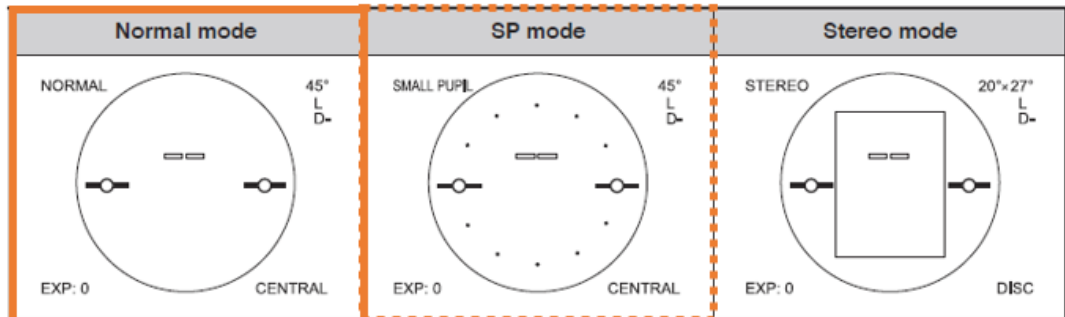
### SWITCH TO RETINAL VIEW

After alignment of the anterior segment is completed, press anterior segment button to switch to retinal observation.

When you want to go back to anterior segment observation, press the button again.



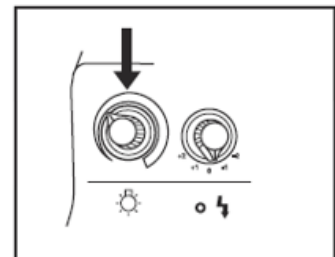
"ANTERIOR" and the pupil diameter aid of the LCD monitor disappear during retinal observation. Anterior segment working dot position aids "(O)" changes to retinal working dot position aids "—", and the focus dots appears.



Adjust the image brightness by retinal observation light intensity control knob when the retinal image, focus dots, and working dots are not clearly shown.

For details of LCD monitor brightness and contrast adjustment, refer to "9.4.6 MONITOR BRIGHTNESS / CONTRAST".

Retinal observation light intensity control knob



## FIXATION INSTRUCTION

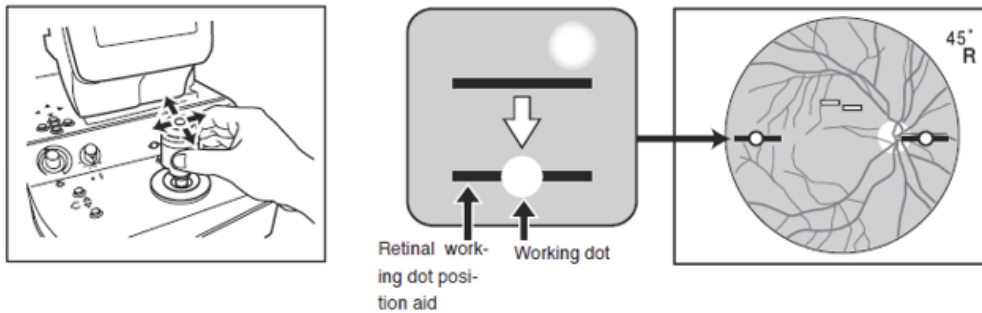
The fixation target position changes when anterior segment observation is switched to retinal observation. In order for the patient to stare at the selected internal fixation target, guide the patient's fixation to the internal fixation target by asking the patient to look at the green light.

Patients would recognize the fixation target at the locations shown in the right table depending on whether the right or left eye is examined and which fixation target position is selected.

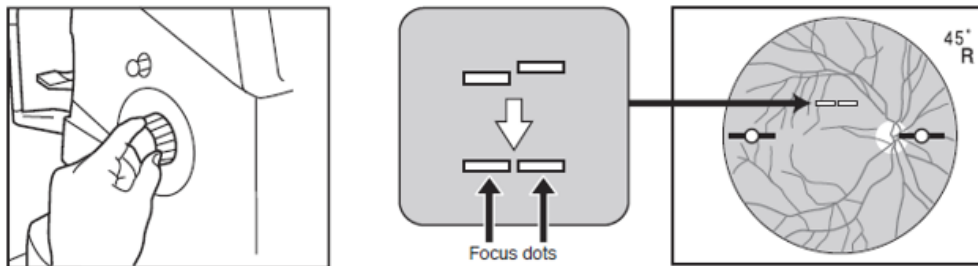
	Right eye	Left eye
Posterior	Near center	
Optic disc	Left	Right
Center of macula	Center	

## ALIGNMENT IN POSTERIOR SEGMENT OBSERVATION AND AQUISITION

Move the optical head base slightly until the sizes of the two working dots become the smallest and the dots are aligned on the top of the left and right retinal working dot position aids "—" in the LCD monitor as shown in the figure below. The focus of the two working dots may be fine tuned by moving the control lever forward/backward.



Turn focusing knob to have two focus dots "—" on the display to form a single line.



After alignment and focusing are completed, photograph by pressing shutter button.

Pictures are automatically stored.








## QUALITY CHECK

Picture quality is controlled on the TV screen. If the quality is considered to be insufficient, a new photograph is taken until satisfactory quality has been obtained.


*Keep in mind the important areas to be analysed in the different photography modes. In photography mode "Normal" with fixation target "Disc", the disc area is critical. In photography mode "Normal" with fixation target "Macula" the macula area is critical. In photography mode "Stereo" with fixation target "Disc", the disc area is critical in both pictures.*

### Dark and white shadows

Examples of retinal photograph	Possible cause	Remedies
Dark shadow or bright reflection appears at the top or bottom of the image. 	The instrument is positioned too high to the patient's eye.  The instrument is positioned too low to the patient's eye.	Perform all alignment steps to obtain a clear retinal image with consistent brightness. Depending on the patient's eye fixation condition, you may obtain a good image by locating working dots away from the dot position aid.
Dark shadow or bright reflection appears at the left or right of the image. 	The instrument is positioned too right or left to the patient's eye.  Diopter compensation knob is not in click.	
Peripheral area become whitened. 	The instrument is positioned too close to the patient's eye. The instrument is positioned too far from the patient's eye.	Locate the digital camera to the position where working dots become smallest. When flares still persist, pull the digital camera a little or move the optical component to the patient. (Working dots may be fades a little.)


The image become whitened locally. 	The objective lens is dirty.	Clean the objective lens. Refer to "10. Maintenance and inspection" for details of the objective lens cleaning.
The lower area become whitened. 	The eyelid or eyelashes intrude the imaging area.	Ask the patient to open his/her eyes wide so that the eyelid or eyelashes do not intrude the area of the pupil, or you or your assistant help the patient keep the eye wide open.

### **Exposure**

Examples of retinal photograph	Possible cause	Remedies
The image is too dark. 	The pupil diameter is small.	Turn exposure compensation knob to +1 or +2 position. If the patient's pupil diameter equal to or smaller than that shown by the working dots, press SP mode button and photograph in SP mode.

If parts of the image is too bright for essential structures to be resolved within the bleached area, reduce exposure to -1 or -2.

### **Sharpness**

Examples of retinal photograph	Possible cause	Remedies
The image is out of focus or blurred. 	The patient has developed a cataract.	Avoiding the area of white turbidity during alignment may allow you to obtain a good image.
	The corneal surface is dry.	Ask the patient to blink before imaging.

If parts of the image is too blurred for essential structures to be resolved within the same area, make sure you have properly alignment (6.1.5. Alignment).

### **SWITCH BACK TO ANTERIOR VIEW**

Repeat protocol for the other eye.

# Annex 3:

## Protocol: OCT

Instrument: Cirrus HD-OCT Model 5000 (Zeiss)

Location: Room 20

### Preparations

#### Switch on the instrument and start Acquisition program

- The acquisition program shall start automatically. If not, click the blue icon on the desktop: "Cirrus HD-OCT"
- Username: *Cirrus Operator*
- Password: (no password)

#### Prepare for use

- Remove lens cap and check clearness of the lens.  
If necessary, use dedicated lens paper and solution to remove stain by gentle rotational movement along a spiral path from centre to periphery of the lens.
- Click "Add New Patient" and enter patient information, or click "Find Existing Patient"

#### Choose sequence of eyes

- Right followed by left or Left followed by right selected from log
- Register and cross out in log
- Acquisition will be in the same sequence for both eyes:
  - Macula: (1) Macular Cube (200x200), (2) HD 1 line 100x (with "EDI"), (3) HD Raster 5 (with "EDI")
  - Optic Disc: (4) Optic Disc Cube (200x200), (5) HD Radial

#### Preparation for imaging

- Clean chin- and headrest with alcohol
- Reduce illumination in room
- Position subject and align head
- Give instructions
- Select patient and click "Acquire" (bottom right on the screen)

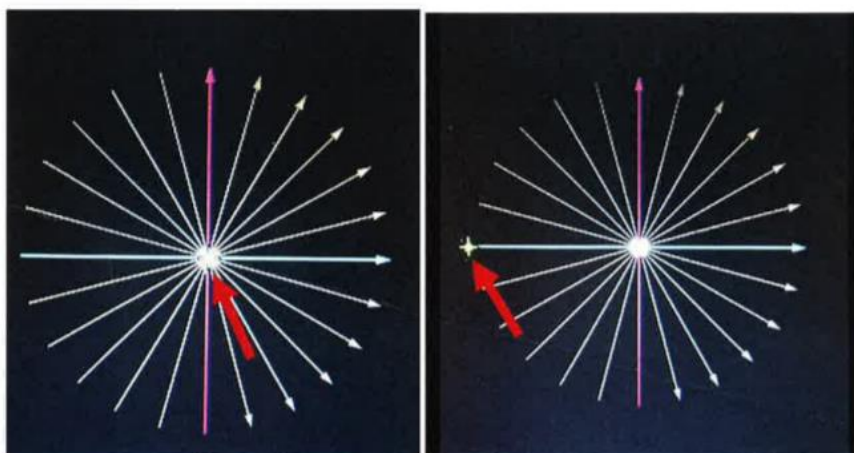
## Acquisition - Optic Disc:

SELECT THE FOLLOWING SCAN MODES FOR SCANS OF THE OPTIC DISC:

- 4) Optic Disc Cube 200x200
- 5) HD Radial

Follow the same instructions as for macular scans. The fixation target for scan number 4) will be automatically moved to one side. Instruct the subject to fixate at the green target before you capture the images.

For scan number 5), make sure that the optic disc is in the centre of the fundus image. If not, move the fixation target by moving the green cross to the side as shown below (red arrows). Make sure that the optic disc is in focus and centred before capturing the images. The white lines, which are the scan patterns, has to be in the centre of the optic disc. Move the scan pattern with by dragging the pattern with the mouse, and position it centrally.



Repeat protocol for the other eye.

## QUALITY CHECK

Make sure that all five scans for both eyes have sufficient quality. Before saving each scan, make sure that the “quality bars” are green.

1 Iris image

2 Fundus image with scan cube overlay with blue and magenta slice navigators

3 Current X slice through front (fast B-scan)

4 Current Y slice through side (slow B-scan)

5 X slices through front and back (fast B-scans)

Check the image quality on the screen. If the quality is considered to be insufficient, a new OCT-scan is taken until satisfactory quality has been obtained.

**Criteria for Image Acceptance:**

**Fundus**

- Make sure that the focus is sharp and clear, good visibility of vessels.
- Scan overlay should be centered on the fovea or optic disc.
- Fundus image should have uniform illumination without dark corners
- There should be no artifacts (or few) that may cast shadow on the OCT scan.
- The OCT *En Face* image should have minimal saccades and no saccades through the area of interest

**OCT**

- OCT scan must be complete in all windows without missing data
- Color density should be the same from end to end.
- Signal strength should be 6 or higher (> 5/10)

## **Annex 4:**

*Protocol: Export and storage of raw images*

To export a raw picture from VK-2/Kowa for storage of raw images

Use the ID-key from Figshare to search.

Database → Open database list... → Search for patient ID → “start search” → double click on selected patient.

Right click once at selected picture/several selected pictures → “COPY” will appear as an icon at the chosen picture in multi view mode. Go to “file” → Export images for study → Select “DATA (D:)” on the password-protected computer as shown in figure below.

A folder with both selected images for RE and LE is created. Change the name on the folder to the ID-number of the patient. E.g.: 1, 2, 3... Change name of picture to e.g.: 1\_OD\_F and 1\_OS\_F, where “1” correlates to the subjects ID-number, “OD” means that it is the right eye, and “F” stands for “fundus photo”.

See figure 3-1 in master thesis.



## Annex 6:

*Protocol: ImageJ (by second observer M.R.)*

OCT-defined beta parapapillary atrophy was defined as an area devoid of retinal pigment epithelium, seen as the upper part of the lowermost hyperreflective complex layer, but with intact Bruch`s membrane, seen as the lower part of the lowermost hyperreflective complex or as a single hyperreflective lowermost layer (when retinal pigment epithelium is lost) (Dai et al., 2013; Hayashi et al., 2012; Kim et al., 2013; Lee et al., 2010; Miki et al., 2017; Miki et al., 2019; Vianna et al., 2016; Zhang et al., 2018).

1. Open ImageJ and upload the IR-image.
2. Change the magnification to 100 percent, and increase the window size, so that the whole image is visible.
3. Change the scale of the IR-image, for concordance between measures in IR-image and cross-sectional image. Go to “Analyze” and “Set Scale...”. Fill in “Distance in pixels”: 642 and “Known distance”: 938 and press OK.
4. Make a circle that is approximately the same size as the papilla, with the borders at the outer edge of the scleral ring. Take the height and width of the circle in pixels and multiply by 0.2. Make a circle with the resulting height and width and centre it in the geometrical centre of the papilla. Include or exclude the cross-sectional images based on the exclusion criteria. Exclude if; centre outside circle, or centre outside papilla.
5. Upload the first included cross-sectional image.
6. Change the magnification to 100 percent, and enlarge the window, so that the whole cross-sectional image can be seen.
7. Reset the scale of the cross-sectional image (make sure this window is the one you are working in), by going to “Analyze” and “Set Scale...”. Press “Click to Remove Scale” and OK.
8. Make a yellow vertical reference line at pixel 469 (half of the whole cross-sectional image of 938 pixels). Go to “Edit” and “Draw” to make the line permanent.
9. If beta parapapillary atrophy is present, measure from the reference line (with the line in the middle of the square) and to the edge of the ending of the retinal pigment epithelium (with the outer edge of the square edge to edge with the ending) on one of the sides of the papilla. Remember the length (pixels) of the measured line.
  - The line should be **yellow**, if the beta zone is present, defined as; ***the area between the end of intact retinal pigment epithelium and the end of Bruch`s membrane.***
  - The line should be **purple**, if there is an overhanging Bruch`s membrane, defined as; denuded Bruch`s membrane which is hanging over the border of

the optic disc, defined as the border tissue of Elshnig. *The main observer (H.K.F.) does not use this marking.*

- The line should be orange if there is gamma zone without beta zone. *The main observer (H.K.F.) does not use this marking.*
- If exclusion or uncertainty, draw a vertical line on the relevant side of the papilla, with colour red or blue, respectively. If the decision of exclusion is changed, make a red cross to include again.

Draw the line by going to “Edit” and “Draw”.

10. Open the IR-image. Make a blue line perpendicular to the respective location (green line in the right degrees) of the cross-sectional image, if uncertain. Make a red line perpendicular to the line of the respective location if excluded. If beta parapapillary atrophy is present, measure the same length as in the cross-sectional image in the same degree-line and mark with a yellow line. If there is overhanging Bruch`s membrane, mark with purple, and orange if only gamma zone is present. Make sure that the square is in the middle of the centre of the scan pattern, and the line thickness should be 1. The line in the IR-image should be the same length as the one in the cross-sectional image +/- 0.5 pixel. Go to “Edit” and “Draw” to make the marking permanent.
11. Repeat step 9 and 10 for the other side of the papilla.
12. Save the cross-sectional image with same filename (ID\_eye\_highest degree number\_lowest degree number), in folder OCT\_scan\_marked, and exit.
13. Repeat step 5-12 for all included cross-sectional images for one eye.
14. Save the resulting marked IR-image with new filename (ID\_eye\_IR\_marked) in folder named OCT-marked, and exit.

## Annex 7:

*Table Annex 7 Distribution of frequencies of “No beta atrophy”, “Beta with certain border”, “Beta with uncertain border” and “Unclassified atrophy” in right and left eye.*

Sections/eye		No atrophy n/N (%)	Beta with certain border n/N (%)	Beta with uncertain border n/N (%)	Unclassified atrophy n/N (%)
0	OD	40/60 (66.7)	11/60(18.3)	0/60(0)	9/60 (15.0)
	OS	27/51 (52.9)	14/51(27.5)	0/51(0)	10/51 (19.6)
15	OD	37/54 (68.5)	11/54(20.4)	0/54(0)	6/54 (11.1)
	OS	29/49 (59.2)	12/49(24.5)	0/49(0)	8/49 (16.3)
30	OD	36/45 (80.0)	6/45(13.3)	0/45(0)	3/45 (6.7)
	OS	29/43 (67.4)	8/43(18.6)	0/43(0)	6/43 (14.0)
45	OD	37/46(80.4)	4/46(8.7)	2/46(4.3)	3/46 (6.5)
	OS	33/43(76.7)	4/43(9.3)	2/43(4.7)	4/43 (9.3)
60	OD	36/40(90.0)	2/40(5.0)	1/40(2.5)	1/40 (2.5)



	OS	32/34(94.1)	1/34(2.9)	0/34(0)	1/34 (2.9)
75	OD	28/30(93.3)	1/30(3.3)	0/30(0)	1/30 (3.3)
	OS	25/26(96.2)	1/26(3.8)	0/26(0)	0/26 (0)
90	OD	18/21(85.7)	1/21(4.8)	1/21(4.8)	1/21 (4.8)
	OS	20/22(90.9)	1/22(4.5)	0/22(0)	1/22 (4.5)
105	OD	18/21(85.7)	1/21(4.8)	1/21(4.8)	1/21 (4.8)
	OS	27/29(93.1)	1/29(3.4)	0/29(0)	1/29 (3.4)
120	OD	27/31(87.1)	2/31(6.5)	1/31(3.2)	1/31 (3.2)
	OS	30/31(96.8)	1/31(3.2)	0/31(0)	0/31 (0)
135	OD	19/22(86.4)	1/22(4.5)	0/22(0)	2/22 (9.1)
	OS	24/26(92.3)	1/26(3.8)	0/26(0)	1/26 (3.8)
150	OD	24/28(85.7)	1/28(3.6)	1/28(3.6)	2/28 (7.1)
	OS	19/20(95.0)	0/20(0)	0/20(0)	1/20 (5.0)
165	OD	37/40(92.5)	1/40(2.5)	1/40(2.5)	1/40 (2.5)
	OS	42/44(95.5)	0/44(0)	0/44(0)	2/44 (4.5)
180	OD	49/52(94.2)	2/52(3.8)	0/52(0)	1/52 (1.9)
	OS	43/45(95.6)	0/45(0)	0/45(0)	2/45 (4.4)
195	OD	49/52(94.2)	2/52(3.8)	0/52(0)	1/52 (1.9)
	OS	42/44(95.5)	0/44(0)	0/44(0)	2/44 (4.5)
210	OD	39/42(92.9)	2/42(4.8)	0/42(0)	1/42 (2.4)
	OS	35/36(97.2)	0/36(0)	0/36(0)	1/36 (2.8)
225	OD	19/24(79.2)	2/24(8.3)	1/24(4.2)	2/24 (8.3)
	OS	18/19(94.7)	0/19(0)	0/19(0)	1/19 (5.3)
240	OD	20/24(83.3)	3/24(12.5)	0/24(0)	1/24 (4.2)
	OS	18/19(94.7)	1/19(5.3)	0/19(0)	0/19 (0)
255	OD	21/24(87.5)	3/24(12.5)	0/24(0)	0/24 (0)
	OS	21/24(87.5)	1/24(4.2)	0/24(0)	2/24 (8.3)
270	OD	18/22(81.8)	3/22(13.6)	0/22(0)	1/22 (4.5)
	OS	16/18(88.9)	1/18(5.6)	0/18(0)	1/18 (5.6)
285	OD	22/28(78.6)	4/28(14.3)	1/28(3.6)	1/28 (3.6)
	OS	28/36(77.8)	5/36(13.9)	2/36(5.6)	1/36 (2.8)
300	OD	32/42(76.2)	5/42(11.9)	2/42(4.8)	3/42 (7.1)
	OS	27/39(69.2)	10/39(25.6)	0/39(0)	2/39 (5.1)
315	OD	32/43(74.4)	7/43(16.3)	1/43(2.3)	3/43 (7.0)
	OS	27/44(61.4)	10/44(22.7)	1/44(2.3)	6/44 (13.6)
330	OD	35/50(70.0)	8/50(16.0)	2/50(4.0)	5/50 (10.0)
	OS	25/43(58.1)	11/43(25.6)	0/43(0)	6/43 (14.0)
345	OD	31/52(59.6)	13/52(25.0)	0/52(0)	8/52 (15.4)
	OS	25/48(52.1)	13/48(27.1)	0/48(0)	10/48 (20.8)

## **Annex 8:**

### **How to use grading scale for total image quality of fundus images:**

*1) Reflect upon and choose the relevant area and structures before taking the fundus image for the clinical purpose. Thereafter, choose the most relevant area within the image for evaluation (e.g. the disc and parapapillary area for follow-up of glaucoma), or evaluate the whole picture (e.g. the disc and macula for screening of diabetes).*

*2) Evaluate sharpness and exposure by the visibility of smallest structures and use the largest capillaries on optic disc especially for sharpness (as presence of capillaries are within all eyes, and a human eye can minimum perceive structures of approximately 20 microns on fundus photo – corresponding to larger capillaries on disc or bundles of RNFL – one can imagine that if the smallest perceivable vessels are detectable, the sharpness is optimal).*

*2.1) Use example images in figure 3-3 for sharpness and figure 3-4 for exposure to decide grading.*

*2.2) Ask yourself if some or all structures are detectable and define whether it's because of sharpness or exposure. Grade according to the scale for both exposure and sharpness.*

*3) Total image quality grade is determined based on the poorest grade for sharpness and/or exposure. Double-check that the criteria for the defined grade of either sharpness or exposure fits with the possibility to do a clinically evaluation of total image quality.*